The heuristic model of energy propagation in free space, based on the detection of a current induced in a conductor inside a continuously covered conducting enclosure by an external radio-frequency source

G Piyadasa[1], UD Annakkage[1], AM Gole[1], AD Rajapakse[1] and U Premaratne[2]

[1]Department of Electrical and Computer Engineering,
University of Manitoba, Winnipeg, Manitoba, R3T 5V6, Canada

[2]Department of Electronic and Telecommunication Engineering,
University of Moratuwa, Katubedda, Moratuwa 10400, Sri Lanka

Email: gamini@codegen.net

(Dated: July 18, 2019)

ABSTRACT

The objective of this study is to propose a heuristic model of energy propagation due to an anomaly; electromagnetic-field penetration into a continuously covered conducting enclosure (Faraday shield) from an external radio frequency source, violating the accepted model in electromagnetic-field theory. In this study, at arbitrarily selected frequency, range of 26.965–1800 MHz, of an external frequency source, an electromagnetic field inside the conducting enclosure was observed, contrary to expectations, which was followed by a systematic examination. Although no induced voltage could be expected inside the enclosure according to classical theory, experiment revealed a clear induced voltage inside; An attenuated induced voltage of -18.0dB to -1.0dB (for the range of frequencies 26.965 – 1800MHz) was observed. Hence these results apparently contradict the established notion that an electromagnetic field cannot penetrate a faraday shield. Rationalizing these observations and the results of the investigation leads to an alternative model to the existing models in energy propagation in free space. In this model, novel quantities named 'ISpin energy' and 'ISpin-energy field' are defined to replace the concept of electric and magnetic fields in classical electromagnetic theory. The proposed ISpin-energy model is capable of explaining the unexpected presence of the electromagnetic field inside the Faraday shield as well as the induction of an alternating current in a conductor placed inside a Faraday shield along with other existing observations in physics such as those in famous Young's double slit experiment on interference of light - which provided the basis for the wave theory.

Keywords: Electromagnetic fields; Faraday shield (cage); electric- and magnetic-field induction; Intrinsic Spin energy; Intrinsic Spin-energy field. δ-spin, λ-spin

Pacs: 03.50.De; 41.20.−q; 41.20.Jb; 74.25.N−; 92.60.Ta; 94.30.Tz

1. INTRODUCTION

As any new revelation has a bearing on accepted existing knowledge, some analysis of the electromagnetic field becomes expedient. The experiments shown here, discuss most fundamental concepts related to the classical electromagnetic field and these fundamental concepts are **recalled** in this introduction with **fine detail to show their contradictory nature** with the observations produced in these experiments. Energy propagation in free space has been described by the wave theory and the quantum theory. Most naturally occurring phenomena have been modelled by using either of these theories [1,2]. In radio-frequency shielding, energy is considered to propagate in the form of electromagnetic (EM) waves, which consist of self-propagating transverse oscillating coupled waves of electric and magnetic fields perpendicular to each other and perpendicular to the direction of propagation of energy. The solutions for linearly polarized planar electric and magnetic fields, *E(r)* and *B(r)*, respectively, at any given point r relative to any arbitrary point in free space are expressed as follows:

$$E(r) = E_0 e^{-ik.r}$$
$$B(r) = B_0 e^{-ik.r} \quad (1)$$

where k is the wave vector normal to the plane of the EM wave, r(x, y, z) is the position vector, E_0 is the amplitude of the electric field, and B_0 is the amplitude of the magnetic field. The behavior of propagating EM waves is mathematically expressed by Maxwell's equations [3,4]. Maxwell's equations describe the electric and magnetic fields arising from the distribution of charges and currents. Maxwell's first equation (Gauss' law) states that the electric flux out of any closed surface is proportional to the total charge enclosed by the surface. The following equation expresses its integral form when a charge *q* is enclosed by a closed surface *A*, resulting in an electric field *E*:

$$\oint \vec{E}.d\vec{A} = \frac{q}{\varepsilon}, \quad (2)$$

where ε is the permittivity of the medium.

The inside of the conducting enclosure cannot contain any charge, as all of the charge exists on the conducting outer surface [4]. Therefore, following Gauss' law and symmetry, the electric field inside the conducting enclosure is zero. In fact, according to Eq. (2), the electric field inside any closed hollow conductor is zero, provided that the region enclosed by the conductor contains no free charge.

As a result, when a time-varying EM wave encounters such a hollow conducting enclosure, according to classical EM theory, two simultaneous mechanisms occur independent of the frequency or wavelength of the incident EM wave.

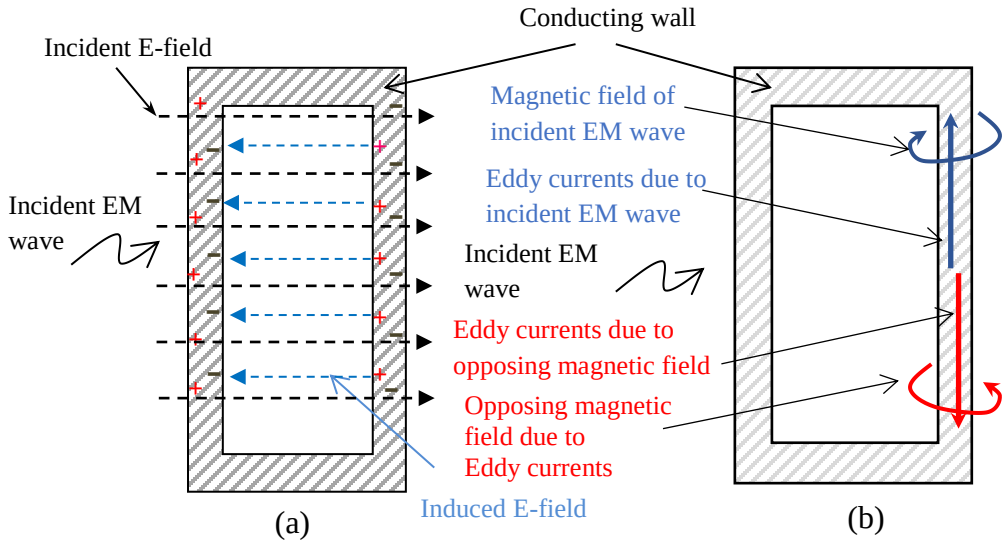

Figure 1. When an EM wave encounters a hollow conducting enclosure, according to the classical theory of electromagnetism, two simultaneous mechanisms occur. (a) The transmitted electric-field component of the EM wave travels through the wall of the conducting enclosure and redistributes free charges in the conducting wall because of induction. An opposing electric field is created by the induced charges on the surface of the conducting enclosure, resulting in zero electric field inside the conducting wall. (b) The incident magnetic-field component (black arrow) induces eddy currents (blue) in the wall of the conducting enclosure. The eddy currents generate an opposing magnetic field (red), canceling the incident magnetic field at the enclosure. Therefore, no magnetic field appears inside the closed conducting enclosure.

1. As shown in Figure 1(a), the transmitted electric-field component of the EM wave travels through the wall of the conducting enclosure and redistributes free charges inside the conducting enclosure by induction. Once an opposing electric field is created by the induced charges on the surface of the conducting enclosure, the resultant electric field inside the enclosure becomes zero [5].

2. As shown in Figure 1(b), the incident magnetic-field component of the EM wave induces eddy currents [5] (blue) due to free charges in the conducting body. The eddy currents generate an opposing magnetic field (red), canceling the incident magnetic field at the enclosure. The resultant magnetic field inside the enclosure is zero. Therefore, no magnetic field appearing inside the hollow conducting enclosure [6].

According to the above-mentioned theory, now established, no electric field or time-varying magnetic field can exist inside a hollow conducting enclosure, and no electric field from outside

can penetrate the enclosure (Figure 1). Such an enclosure is called an EM shield or Faraday shield [7].

Summarizing, in a faraday shield, the EM wave separately (not bounded together) exerts two individual forces (due to electric and magnetic fields) on the surface of the enclosure and produces a net zero EM field in the interior of the conducting enclosure (Figure 1).

The Faraday shield concept is widely applied by present-day industry for shielding instruments and processes from EM interference (EMI) [8,9] such as medical instruments, analytical instruments, and electronic and communication systems. However, it is important to note that all the instruments and implements used inside the Faraday shield are strictly grounded to the Faraday shield itself to provide proper shielding. This is the most important criterion in the present-day use of a Faraday shield [6]. However, according to the working principle of the Faraday shield, there should be no need for the instruments used inside the shield to be connected to the Faraday shield and grounded, as there is no EM field that can penetrate the shield from external sources [5]. Moreover, there is evidence showing that, even when the grounding technique is utilized, the EM field still continues to exist inside the Faraday shield [10-12].

If a field due to an external EM source exists/penetrates inside a Faraday shield, the present theory suggests that either the enclosure is not perfectly closed because of apertures (for example, holes in the enclosure) or the enclosure is completely closed but the wall is too thin to provide adequate shielding.

In the case of an imperfect enclosure, the penetration depends on the size of the openings. The case in which the conducting enclosure has openings facing the emission of radiation, has been extensively and rigorously studied elsewhere [13-16]. According to EM field theory, EM waves do not penetrate very far through holes that are significantly less than a wavelength across [13,17]. Equivalently, the reflection of EM waves from a conducting surface is not affected by holes (or other irregularities) on the surface that are significantly less than a wavelength across. Therefore, a Faraday shield (in this case, it is commonly known as a Faraday cage even when such holes are present on the surface) or an antenna reflector is constructed by using a metallic wire mesh (with a spacing that is small compared to the wavelength) without a drastic compromise in performance. It is important to note that the commonly referred Faraday cage is not essentially a continuous covering, as it may contain openings. **In this paper, only continuously covered conducting enclosures (i.e. without openings) are considered and referred to as Faraday shields.**

As discussed above, when holes exist on an imperfect metal surface, the penetration of EM waves through these holes depends on the incident frequency. The incident frequency is categorized into high-, intermediate-, and low-frequency regions relative to the dimensions of the holes on the surface [18]. If a hole is large compared to the incident wavelength, it is considered a high-frequency region, and EM waves pass freely through the hole (i.e., aperture). Many of the laws in

physical optics are applied under this assumption. Resonance occurs (aperture excitation) [19] when the aperture dimensions are approximately equal to the wavelength, and the respective frequencies are considered as being in the intermediate-frequency region. In the low-frequency region, where the aperture is small compared to the wavelength, the laws of Kirchhoff-Fresnel [20-24] diffraction or boundary diffraction (BDW) [25-28] can be applied to analyze the field distribution.

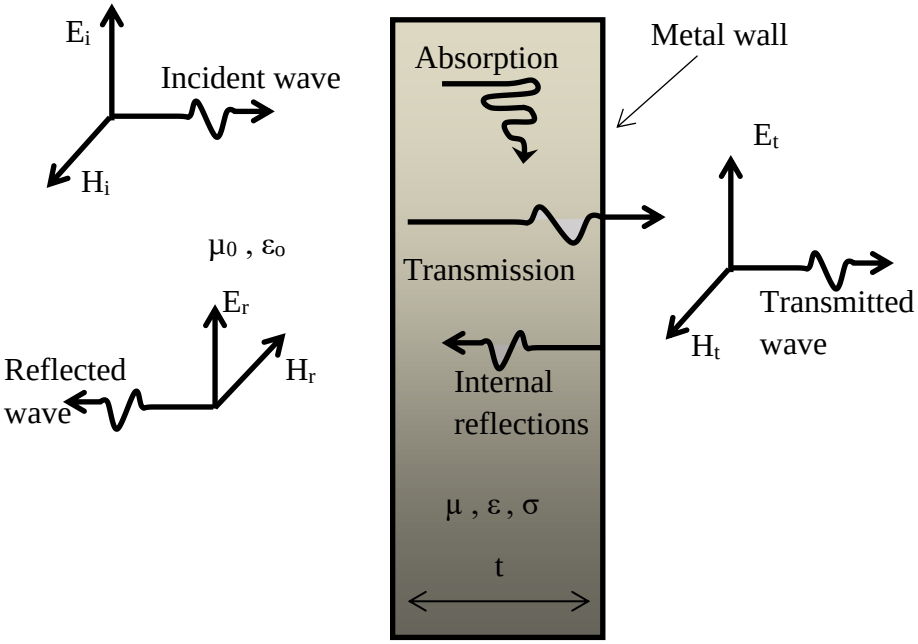

Figure 2. EM shielding. When an EM wave is incident on a metal wall of thickness t, the EM energy is partially reflected and partially absorbed by the metal wall. Some of the EM energy penetrates the metal wall depending on the thickness t, permeability μ, permittivity ε, and conductivity σ of the wall. The electric- and magnetic-field components of the incident, reflected, and transmitted waves are (E_i, H_i), (E_r , H_r), and (E_t, H_t), respectively.

In case of a thin wall, the EM field can be transmitted through and can appear inside the Faraday shield (Figure 2) [18,29-32]. When an EM wave with an energy I_{dB} is incident on a metal wall of thickness t, the EM energy is partially reflected (R_{dB}) and partially absorbed (A_{dB}) by the metal wall. Some of the EM energy penetrates (T_{dB}) the metal wall depending on the thickness t, permeability μ, permittivity ε, and conductivity σ of the wall. The energy conservation when an EM wave is incident on a conducting wall is expressed by Eq. (3), and the shielding effectiveness (SE) is defined by Eq. (4):

$$I_{dB} = R_{dB} + A_{dB} + T_{dB}, \tag{3}$$

$$SE = I_{dB} \Big/ T_{dB}. \tag{4}$$

SE can be determined when the reflection losses (R_{dB}) defined by Eq. (5) and absorption losses (A_{dB}) defined by Eq. (6) are known [31] for a given I_{dB}:

$$\text{Reflection losses} = R_{dB} = 168 + 10\log_{10}\left(\frac{\sigma}{\mu f}\right), \tag{5}$$

$$\text{Absorption losses} = A_{dB} = 131.4t\sqrt{f\mu\sigma}, \tag{6}$$

The *SE* through a conducting wall is considered as two separate components, as in the case of a Faraday shield (Figure 1): the electric-field shielding effectiveness (SE_E) and magnetic-field shielding effectiveness (SE_M). The shielding effectiveness for electric and magnetic fields is defined as the ratio of the field magnitude at a point without and with the metal wall [31]:

$$\begin{aligned} SE_E &= 20\log_{10}\left|\frac{\hat{E}_i}{\hat{E}_t}\right| \\ SE_M &= 20\log_{10}\left|\frac{\hat{H}_i}{\hat{H}_t}\right| \end{aligned}, \tag{7}$$

where E_i and E_t are the electric fields of the incident and transmitted waves, respectively. The incident and transmitted magnetic fields are given by H_i and H_t, respectively.

The value of E_i/E_t can be calculated as follows:

$$\left|\frac{\hat{E}_i}{\hat{E}_t}\right| \cong \left|\frac{\eta_0}{4\hat{\eta}}\right| e^{t/\delta}, \tag{8}$$

where η is the radiation impedance of the medium. For a conducting enclosure, the atmospheric conditions are roughly equivalent to those of free space. Therefore, $\eta \approx \eta_0 \doteq \sqrt{\frac{\mu_0}{\varepsilon_0}}$, where μ_0 and ε_0 are the permeability and permittivity of free space, respectively.

The impedance of the conductor, $\hat{\eta}$, is approximated as follows:

$$\hat{\eta} \approx \sqrt{\frac{2\pi f \mu_r \mu_0}{\sigma}} < \frac{\pi}{4}. \tag{9}$$

Since $\frac{\sigma}{2\pi f \varepsilon} \gg 1$ (ε is the permeability of the conductor)**,** SE_E is considered equal to SE_M when the radiation source is kept at a far field from the metal wall. However, for the near field, where the radiation source is in the vicinity of the metal wall, SE_E and SE_M are not considered equal [6,31].

With a higher electrical conductivity, when the frequency of the incident wave increases, most of the EM energy is concentrated near the surface of the metallic enclosure because of eddy currents. This also causes negligible EM fields inside the enclosure (Figure 1). This is known as the skin effect [33,34], and the skin depth δ describes the depth to which radiation can penetrate the shield. The skin depth is expressed as follows:

$$\delta = \sqrt{\frac{2\rho}{(2\pi f)(\mu_0 \mu_r)}}, \tag{9}$$

where $\boldsymbol{f}$ is the frequency of the incident EM wave, $\boldsymbol{\mu_0}$ is the absolute magnetic permeability, ρ and $\boldsymbol{\mu_r}$ are the conductivity and the relative permeability of the conducting material respectively.

In addition to the electrical conductivity (σ) and permeability (μ) of the conducting material, the dielectric absorption and surface porosity of the enclosure affect the penetration and reflection of EM waves [35].

The electric field in a Faraday shield, irrespective of the shape of the enclosure [5], due to an externally applied **electrostatic field** has been explained similarly to that due to a time-varying electric field. For an external **static magnetic field**, the shielding depends on the permeability of the material and the shape of the conducting enclosure [4].

However, the formation of a zero-EM field within a Faraday shield due to the individual actions of the electric and magnetic fields relevant to the classical EM wave theory has not been adequately studied. To address this shortcoming, the following experiments were designed to investigate the shielding process within a Faraday shield at randomly chosen frequencies (26.965, 151.880, 500, 900, and 1800 MHz). The voltage signals due to induced currents in a simple monopole conductor were examined with and without a Faraday shield (constructed with a 1.2-mm-thick copper sheet).

The above experiment has clearly indicated the presence of electric and magnetic fields inside the Faraday shield (details are discussed later in this manuscript), contradicting the existing understanding of this phenomenon, which predicts a zero EM field inside the Faraday shield by the reasoning that free electrons in the metal redistribute themselves dynamically to create a counteracting EM field that cancels the internal field. According to the classical theory, the zero EM field inside a Faraday shield is described by the fundamental aspects of electric and magnetic fields, and the zero field completely depends on the free charges (electrons) of the metal. This fact

leads to a contradiction if those free charges are bounded and immobilized by another strong external electric field. In this situation, free charges would not be available for creating a zero EM field, and an external EM field should appear inside the Faraday shield. This aspect is out of the scope of this manuscript and to be discussed separately.

Hence, the E-field detected inside the faraday shield cannot be explained by the existing theory. Subsequent observations made using appropriate experimental setups (detailed in Section II) also led to the new model of energy propagation in free space.

Experiments showing the presence of energy fields that can induce a current in a conductor placed inside the Faraday shield are presented in Part-A of this paper. Thus, these experiments have convincingly revealed an energy field inside a faraday shield. Further, the observation that an induced current can arise in a conductor inside Faraday shield confirms the above fact: A Faraday shield can sustain an E-field inside it. Hence an alternative theory for propagation of energy is called for.

In Part-B, to explain our observations, an alternative heuristic model has been proposed for the propagation of energy in free space. In this model, new quantities named "ISpin-energy" (Intrinsic Spin Energy or ISpE) and "ISpin-energy field" (Intrinsic Spin Energy Field or ISpEF) are defined to replace the role of electric and magnetic fields in the classical EM wave theory.

PART A

II. METHOD

1. Primary study of field penetration

In order to detect if a signal is present within the Faraday shield, an antenna and a receiver were placed inside a Faraday shield, as shown in Figure 3. Two similar copper cubic enclosures (CuCuE) of dimensions 55 cm x 55 cm x 55 cm were carefully built based on standard shielding methods [36] preventing EM-field leakage. Copper sheets of 1.2-mm thickness were used for the construction. One chamber was built by soldering using Sn/Pb (63:37) to reduce cold solder joints, and the other was built with copper TIG welding. Both chambers showed similar results throughout the experiment. Therefore, no discussion is made on the construction technique which is irrelevant.

The CuCuE shield was irradiated with external EM sources at frequencies of 26.965 (1111 cm), 151.880 (200 cm), 500 (60 cm), 900 (33 cm) and 1800 (16.7 cm) MHz. For 26.965, 151.880, and 500 MHz, a tuned RF power meter was used to measure the field inside. For 900 and 1800 MHz, the commercial GSM900 and GSM1800 signals were used, respectively. GSM mobile phones installed with applications for signal-strength measurements were used as receivers. The voltage

signals due to induced currents in a simple monopole conductor were measured with and without a Faraday shield in place. The results are discussed in section III. As a significantly strong signal was detected contrary to the classical EM theory interpretation within the CuCuE at all frequencies, a further detailed experiment was designed to investigate the field detected within the Faraday shield.

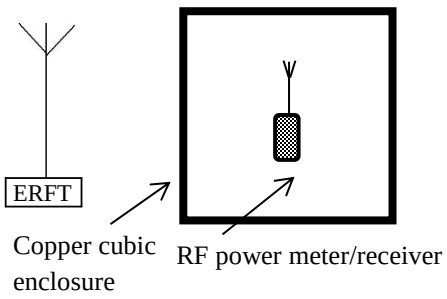

Figure 3. Experimental setup I: A copper box of dimensions 55 cm x 55 cm x 55 cm (1.2-mm thickness) was irradiated with radio frequencies of 26.965, 151.880, 500, 900, and 1800 MHz. A device for measuring signal strength was placed inside the chamber.

2. Detailed study of field penetration

In this experiment, only a single source of frequency 151.880 MHz was selected arbitrarily.

Experiment Apparatus

1. Two monopole antennae (410-mm long)
2. One square-loop antenna (410 mm x 40 mm)
3. As shown in Figure 4, a closed Faraday shield was made using a 1.2-mm-thick copper sheet with a circular base of 50-mm diameter and approximately 420-mm height. To measure voltage signals due to induced current in the antenna inside, two holes of 10-mm diameter were made on the circular base for the Bayonet Neill–Concelman (BNC) connectors. This design of the Faraday shield is named as a copper cylindrical enclosure (CuCyE).
4. Two separate battery-operated digital oscilloscopes (Tektronics TPS 2024) having four isolated channels were used for voltage measurements. In an isolated channel oscilloscope, each channel has its own ground, and these ground terminals were not connected to each other.
5. 2 W/151.880 MHz vertically polarized sinusoidal signal source
6. Equal-length 50-Ω coaxial cables

The dimensions of antennae and CuCyE were selected to be close to the quarter wavelength of the source frequency of 151.880 MHz. Two separate digital oscilloscopes were used in order to minimize the coupling between antenna measurements. The transmitting antenna was a 0.5 m quarter-wavelength vertical telescopic monopole antenna. The experiment was performed under general indoor propagation conditions. The transmitter was placed 8 m away from the Faraday shield.

To synchronize the two measurements, the trigger inputs of the two oscilloscopes were fed with signals induced by a single 151.880 MHz signal in two separate antennae (see Supplementary data Note 1. Sup. Fig. 1). Both antennae were placed approximately the same distance away from the 151.880 MHz source. Observations made with two oscilloscopes were similar to those made with two separate isolated channels, CH1 (with its ground_{CH1}) and CH2 (with its ground_{CH2}), of a single oscilloscope. Therefore, two separate isolated channels of a single oscilloscope were used when the magnitudes and phases were measured simultaneously for two signals. In the experiments, the induced currents at the antennae were measured as voltage across the input impedance (1 MΩ) of the oscilloscope.

The near-field distance from the transmitting antenna is approximately equal to $2L^2/\lambda$ [37], where L is the highest length of the antenna. This yields a near-field distance of 1.5 m. Therefore, as the distance between the source and antenna was 8 m, the near-field behaviors of EM waves can be excluded in this study.

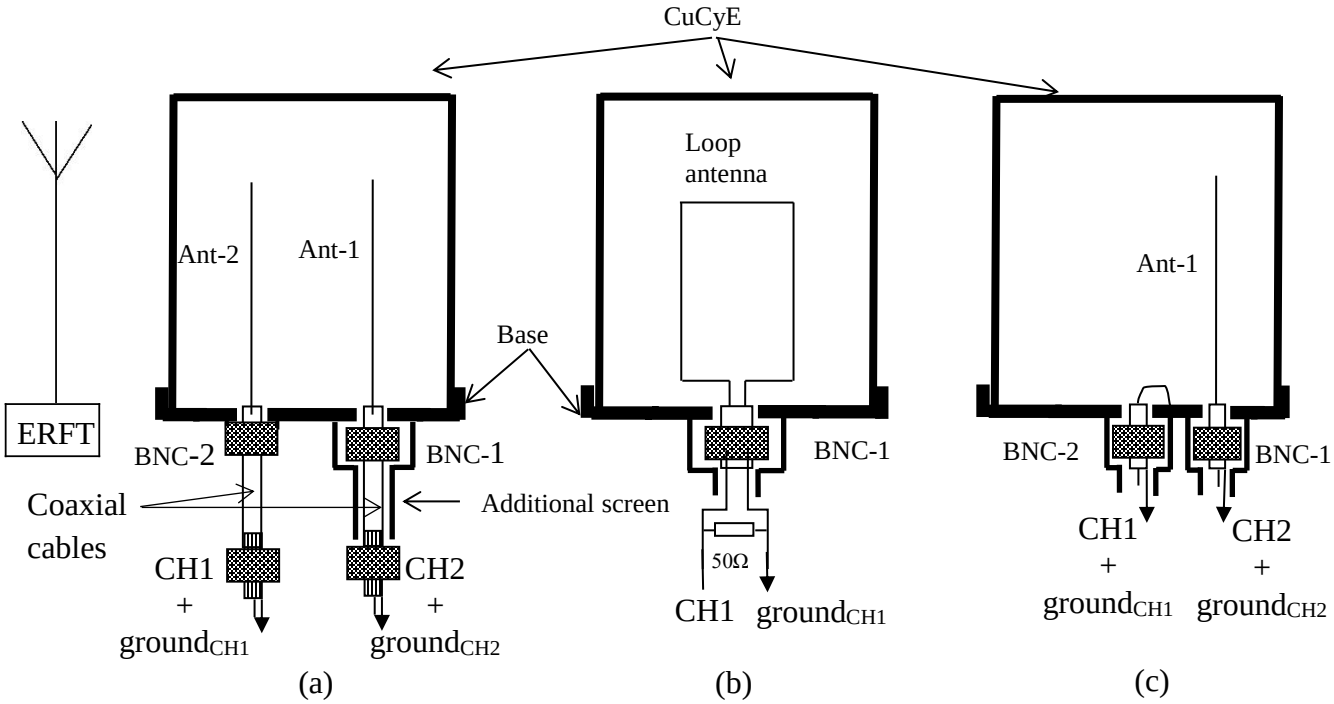

Figure 4. Experimental setup II: (a) Two monopole antennae, Ant-1 and Ant-2, were connected to a digital oscilloscope using two equal-length coaxial cables. The outer shields (oscilloscope ground) of the coaxial cable from CH2 was not connected to the CuCyE at BNC-1. However, an additional shield was made at the BNC-1 in order to restrict possible field penetration in to CuCyE. (b) To determine whether a time-varying magnetic field exists inside the copper enclosure, a rectangular wire loop antenna shunted by a 50-Ω resistor was placed inside the enclosure. (c) Ant-1 and the CuCyE were separately connected to the oscilloscope using coaxial cables. In Exp. II(c), the outer shields (oscilloscope ground) of both coaxial cables were not connected to the CuCyE. Connections to the antenna and the CuCyE were made through an insulated BNC.

The following three experiments were performed.

Exp. II(a). Two monopole antennae, Ant-1 and Ant-2, were placed inside the CuCyE and connected to oscilloscopes CH2 and CH1, respectively, via BNC connectors. The screen of the coaxial wire to Ant-1 was connected to the oscilloscope ground_{CH2} **but it was not connected to the CuCyE** (an isolated connector, AMP 112431, was used for BNC 1). The screen of the coaxial wire of Ant-2 was connected to the oscilloscope ground_{CH1} as well as to the CuCyE via BNC 2 (AMP 227755-1). As shown in Figure 4(a), the cable end connected to BNC 1 was additionally screened by a copper foil in order to restrict possible EM penetration in the CuCyE through the gap. The gap between the CuCyE and the outer coaxial screen of the insulated BNC 1 was approximately 0.2 mm. Two voltage measurements from Ant-1 and Ant-2 were taken without the shield, CuCyE (only the base, after removing the CuCyE; see Supplementary data, Note 2 (Sup. Fig. 2) and with the shield (antennae enclosed with the CuCyE, as shown in Figure 4(a)). The 151.880-MHz signal source was used to create a field at the CuCyE. Exp. II(a) was repeated with six (6) isolated enclosures (enclosures within enclosures) but only with Ant-1: the details and results are provided in the Supplementary data (Supplementary data, Note 3 and Sup. Fig. 3). Ant-1 and Ant-2 were also shielded with multiple configurations: the details of which and the results are provided in the Supplementary data (Notes 4 & 5 and Sup. Fig. 4 & 5).

Exp. II(b). This experiment was performed to determine whether a time-varying magnetic field existed inside the CuCyE. The two antennae were replaced by a rectangular wire loop antenna shunted with a 50-Ω resistor, as shown in Figure 4(b). Oscilloscope CH1 and its ground_{CH1} terminals were directly connected to the two ends of the wire loop, as shown in Figure 4(b). As in Exp. II(a), the unshielded and shielded voltage measurements were taken when the 151.880-MHz signal source creates a field at the CuCyE.

Exp. II(c). The third experimental setup is shown in Figure 4(c) and uses a single enclosed antenna. Ant-1was connected to oscilloscope CH2 as in Exp. II(a). The housing of the CuCyE was independently connected to oscilloscope CH1 using coaxial cable as shown in the Figure 4(c). **Note that,** the outer shields (oscilloscope grounds) of both coaxial cables were not connected to

the CuCyE. Again, the 151.880-MHz external signal source was used to create a field at the CuCyE.

For each experiment, in order to observe the impact of noise, the signals induced in the cables connected to the CuCyE were measured without the antennae (Supplementary data, Note 6 Sup. Fig. 6). The 151.880-MHz external signal source was in operation when the measurements were taken. In addition, the experiments were repeated with the CuCyE grounded to the actual ground as well as electrical ground of the main power supply.

Finally, the experimental setups were simulated using Ansys High Frequency Structural Simulator (HFSS) 13.0.0, and the results of the experiments and respective simulations were compared.

III. RESULTS

Table I summarizes the results of the primary study of field penetration. For frequencies of 26.965, 151.880, 500, 900, and 1800 MHz, the power induced in the monopole conductor without and with the CuCuE (Figure 4) are tabulated in Table I, where the signal strength is given in dBm.

TABLE I. Signal strength measured in dBm without and with the copper enclosure for frequencies of 26.965, 151.880, 500, 900, and 1800 MHz.

Frequency (MHz)	Wavelength (cm)	Signal strength (dBm)		Signal source OFF (dBm)	S_w/S_{wo} (dB)
		Without CuCuE (S_{wo})	With CuCuE (S_w)		
26.965	1110	-10	-28	~ -59	-18.1
151.880	200	-29	-36	~ -59	-7.0
500	60	-23	-31	~ -59	-8.0
900	33.3	-96	-97	n/a	-1.0
1800	16.7	-97	-98	n/a	-1.0

For the selected frequencies within the 26.965-1800 MHz band, the calculated ratio between the measured voltage due to the induced current at the antenna without the CuCuE to that with the CuCuE is in the range of -18.1 dB to -1.0 dB. The data in Table I also indicate that the signal inside the conducting CuCuE increases with the decrease of wavelength relative to the dimensions of the CuCuE. At 1800 MHz, the effect of the Faraday shield is very small in the observed

frequency range. Most interestingly, the results confirmed that EM energy penetrates walls and exists within the CuCuE, contradictory to the classical interpretation of the Faraday shield.

The observed voltage waveforms in the detailed study of field penetration are shown in Figures 5 and 6. Figures 5(a) and 5(b) show two waveforms obtained from Exp. II(a). Figure 5(a) shows the voltage due to induced currents in antennae without the shielding (see Sup. Fig. 1), while Figure 5(b) shows the voltage signals when the antennae were shielded by the CuCyE. The blue (CH2) and yellow (CH1) waveforms in the figures show the induced voltages in Ant-1 and Ant-2, respectively. Figures 5(c) and 5(d), respectively, show the measured voltage due to induced current in the loop antenna without and with the CuCyE. The measured voltages in Exp. II(a) and Exp. II(b) are summarized in Table II.

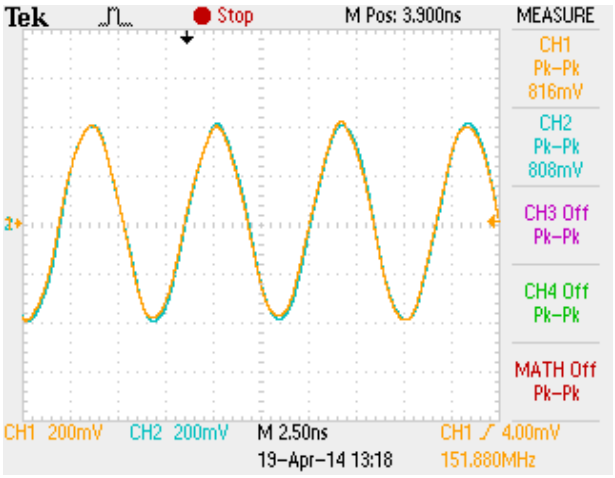

(a)

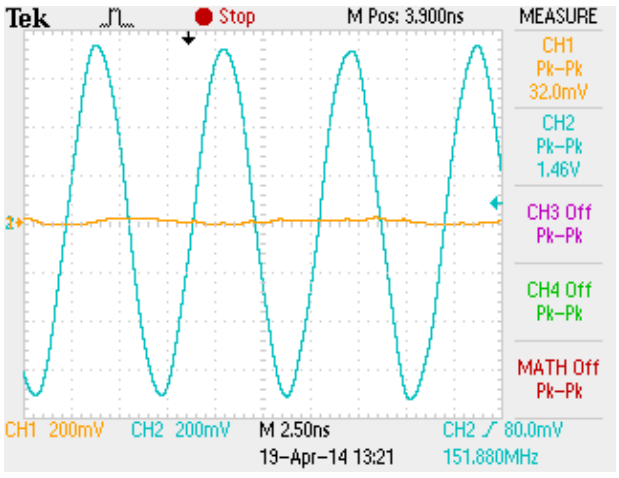

(b)

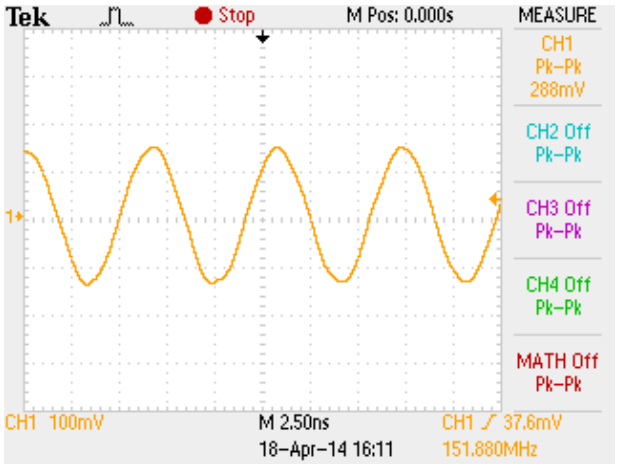

(c)

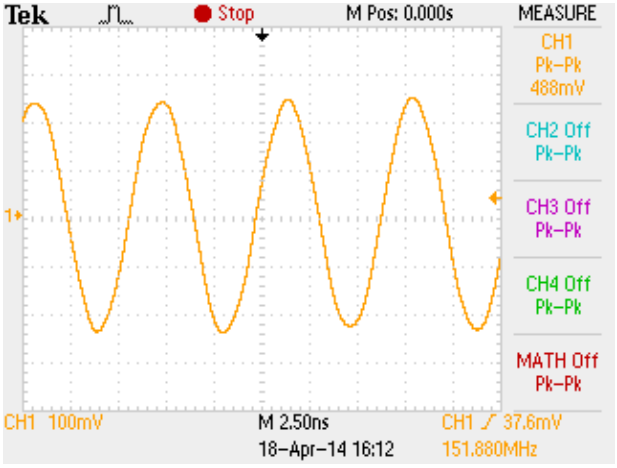

(d)

Figure 5. Measured voltage signals from antennae in Exp. II(a) and II(b). (a) Measured voltages from unshielded antennae. (b) Voltage measurements when the antennae were shielded with the CuCyE. (c) Measured voltage in the loop antenna without the CuCyE. (d) Measured voltage in the loop antenna shielded with the CuCyE.

TABLE II. Induced voltages at Ant-1, Ant-2, and the loop antenna

	Exp. II(a) voltage (mV)		Exp. II(b) voltage (mV)	
Antenna	without CuCuE	with CuCuE	without CuCuE	with CuCuE
Ant-1	816	1460	-	-
Ant-2	808	32	-	-
Loop	-	-	288	488

Figure 6 shows the measured voltages due to induced currents in the antenna and the copper enclosure CuCyE in Exp. II(c). The measured voltages are approximately equal in magnitude (488 mV) and in phase.

Prior to attaching antennae, the voltage captured by coaxial cables connected to the CuCyE were approximately 24 mV (see Note 6 and Sup. Fig. 6). No measurement in any experiment is altered when CuCyE is connected to the actual ground and the electrical ground of the main power supply.

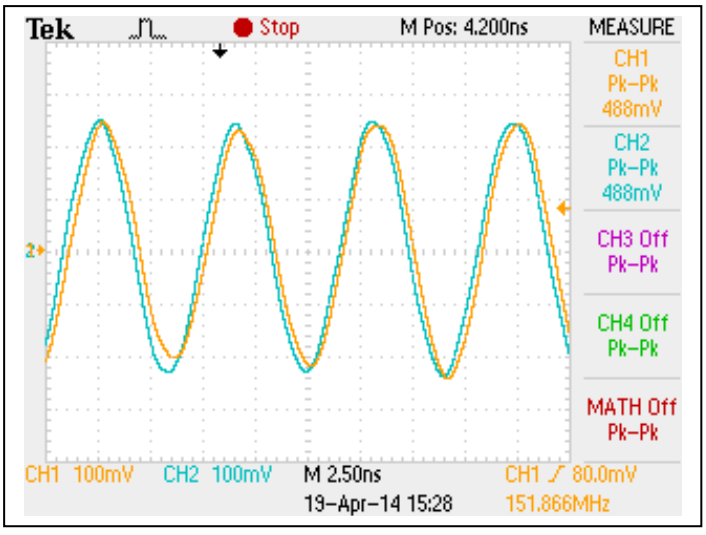

Figure 6. Voltage measured in Exp. II(c). The voltages in the antenna and CuCyE were approximately equal in magnitude (488 mV) and in phase.

Exp. II(a) was simulated using Ansys HFSS, and the results are shown in Figures 7 and 8. The simulation results were compared with the experimental results. X and Y are considered local ground terminals of the oscilloscope channels CH2 and CH1, respectively. X' and Y' are considered the connecting terminals (signal feeding points) (BNC 1 and BNC 2) of the antennae to the oscilloscopes CH2 and CH1, respectively. The electric fields between XX' or YY' simulated by Ansys HFSS are assumed to be proportionally representing the voltage signals produced in CH2 (with reference to the $ground_{CH2}$) and CH1 (with reference to the $ground_{CH2}$) of the oscilloscope owing to the induction of currents in Ant1 and Ant2, respectively. In the case without the CuCyE (Sup. Fig. 2), as shown in Figures 7(a) and 8(a), the presence of a field near the two antennae can be observed from the electric-field distribution along the *XX'* and *YY'* gaps. The simulated gap is 10 mm. The electric field across the gap estimated using the results of simulation was 52 V/m. The voltages correspond to the electric-field distributions shown in Figure 8(a) (approximately 520 mV = 52 V/.01m) and are comparable to the measured voltage due to induced current at two monopole antennae (approximately 800 mV, as indicated in Table II and Figure 5(a)). However, with the CuCyE, the simulation results are contradictory to the experimental observations. Although the voltage was measured at Ant-1 in the experiment, as shown in Figure 7(b) and the contour plot in Figure 8(b), no electric field was observed across the gap in the simulation results. The experimental observation showed a voltage of 1460 mV (Figure 5(b) and Table II) instead of the value 0 V/meter predicted by the simulation.

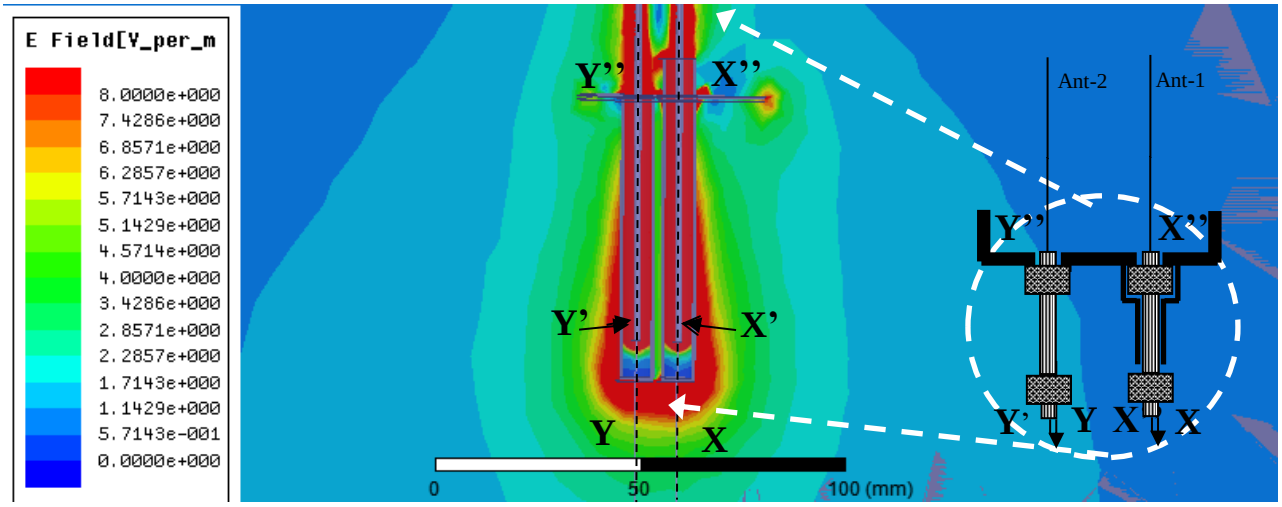

(a)

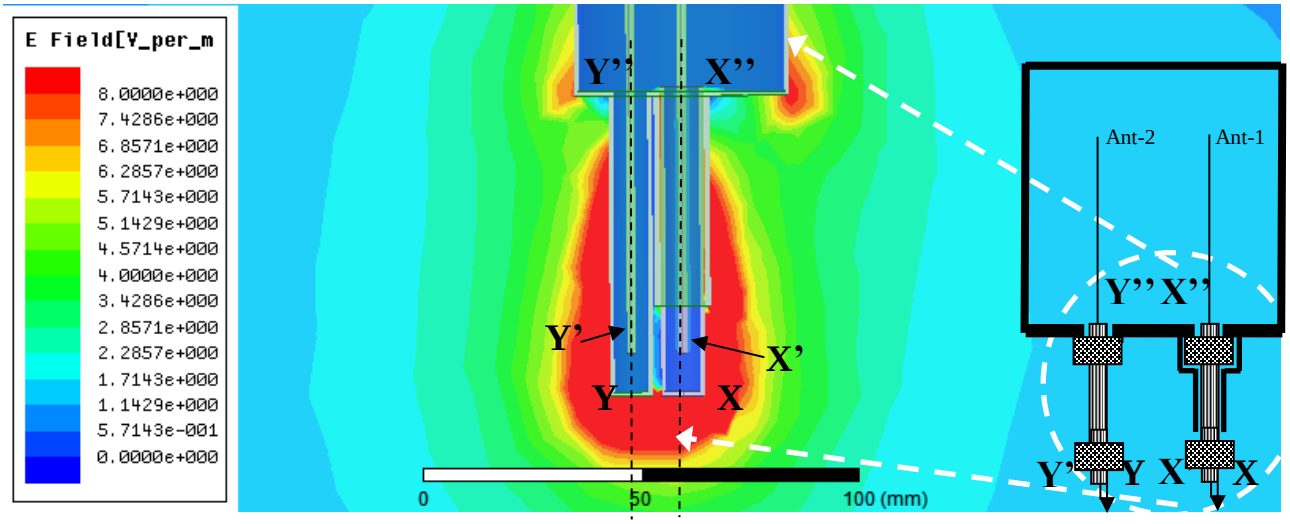

(b)

Figure 7. Contour plots of the simulated EM field. (a) Electric-field distribution without the CuCyE. The geometry of the experimental setup is shown on the right side. The points X, X', and X'' (Y, Y', and Y'') represent the oscilloscope ground, voltage signal (feeding point) input to the oscilloscope, and voltage signal input to the coaxial cable from the antenna through the BNC, respectively. (b) Electric-field distribution with CuCyE.

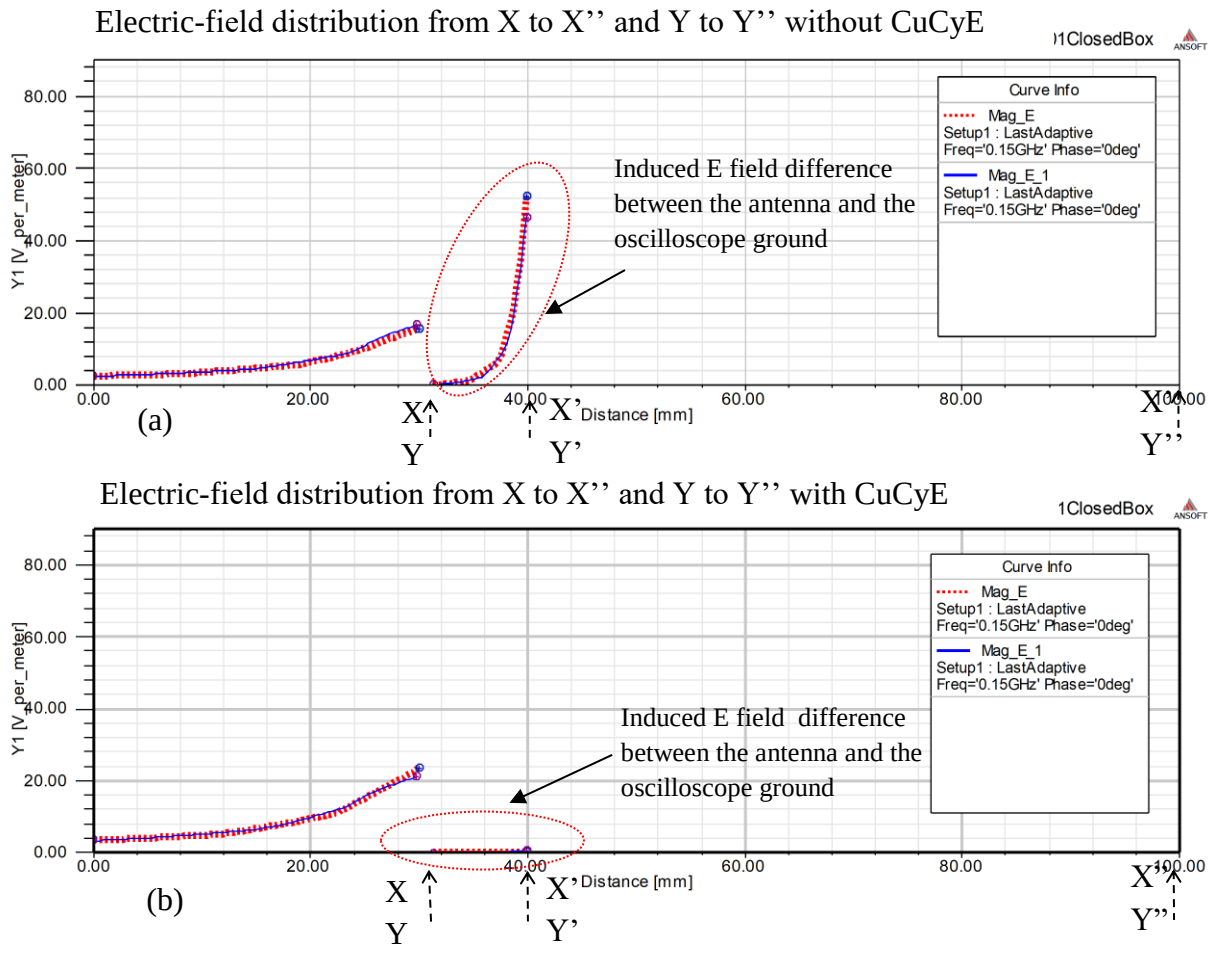

Figure 8. Induced electric-field distribution along the axis of the two monopole antennae. (a) Without CuCyE, the electric-field differences between the oscilloscope ground and both antenna outputs (XX' and YY'') are nearly 52 V/m. (b) With the CuCyE, the electric-field differences between the oscilloscope ground and both antenna outputs are negligibly small.

IV. DISCUSSION

The classical theory states that a variation in EM field can induce a current in a conductor. According to classical theory, when such a field encounters a Faraday shield, it is reflected/absorbed, and no EM field appears inside the shield. In this study, we experimentally detected the presence of an energy field using an antenna placed inside a Faraday shield, contradicting the explanation provided by the classical theory (Figure 1(a)). The results in Table 1 clearly show that the signal penetrates the CuCuE and is detected within at all wavelengths tested. However, the detected signal weakened with increasing wavelength (or decreasing frequency).

The presence of a voltage signal in the oscilloscope, when it is connected to an antenna, indicates the presence of an energy field at the location of the antenna. An electrically floating (battery operated), isolated channel oscilloscope facilitates the two measurements of voltage signals simultaneously and independently, as with two separate oscilloscopes, but with a common trigger input signal. The ground terminals of each channel are also electrically isolated from the other. Therefore, in the simultaneous measurements, the ground references are independent. The measurement of two signals simultaneously and independently is the most crucial feature in this experiment used to resolve the field inside the Faraday shield.

To elaborate on this topic further, to measure any physical quantity, a reference has to be defined. The oscilloscope or any other measuring equipment measures a signal relative to a reference created by the signal itself, rather than set by the measuring device [38]. If there is no such reference, then the measurement cannot be made. The EM wave is a part of a system (frame of reference) different from the system in which the measuring instrument exists. Therefore, the signal itself must induce a reference at the oscilloscope ground, but this induced reference needs to be different from the signal in the antenna in order to detect/measure the signal. There will be no signal detected if the signal induced in the antenna is identical to the signal induced in the reference (common mode signal).

According to the working principle of the Faraday shield, there should be no need for the instruments used inside the shield to be connected to the Faraday shield, as no EM field from external sources can penetrate the shield [5]. However, to date, whenever the possibility of an EM field penetrating a Faraday shield was explored, the detectors used inside were grounded to the Faraday shield, and zero voltage observed inside the Faraday shield was due to the groundings. Figure 6 shows that a voltage measured because of the induced current in the CuCyE is nearly equal in magnitude and phase to the voltage measured in the antenna inside the CuCyE (Figure 4(c)). An oscilloscope measures the signal with respect to its own ground reference. If the ground of an oscilloscope is connected to the CuCyE, since the CuCyE and Ant-2 are at the same voltage at any moment in time, there is no resultant output voltage. For the same reason, a zero voltage is observed in Ant-2 in Exp. II(a), as the oscilloscope ground reference is connected (via the shield of the coaxial cable) to the CuCyE (Figures 4(c) and 6). These results undoubtedly imply that the currents are induced in both antennae, Ant-1 and Ant-2. However, Ant-2 does not produce a voltage signal at CH1 in the oscilloscope, as its reference is also connected to the same voltage variation at the Faraday shield (CuCyE), resulting in a net zero output at the oscilloscope. Ant-1 produces a voltage signal at CH2 in the oscilloscope, as its reference is floating (Figure 4(a) and 5(b)) and free to induce a reference voltage signal due to the same EM wave that produces current in the ANT-1.

In Exp. II(a), the measured signal at Ant-1 was 816 mV (without the shield) without the oscilloscope ground connected to the base of the CuCyE. In the case of Ant-2 with the coaxial cable shield connected to the base, the reading was 808 mV (without the shield). Hence, nearly

equal signal amplitudes can be measured in both antennae without the CuCyE (Figure 6(a) and Supplementary Figure 1). This is also confirmed by the HFSS simulation in Figure 8(a). When two antennae were completely enclosed by the CuCyE, a considerable voltage gain (from 816 mV to 1460 mV) was observed at Ant-1, (where the screen of the coaxial cable, the oscilloscope ground, was not connected to the CuCyE). However, as shown in Figure 5 (b), the signal strength of Ant-2 was reduced and it was closed to the background noise level (32 mV). The noise recorded in CH1 and CH2 was only 24 mV when the antennae are not connected to the end of the coaxial cable in the CuCyE (see Supplementary data Note 6 and Sup. Fig. 6). This **background noise level** implies that the measured signals **which were far more greater, in the experiments** were always due to the induction of currents in Ant1 and Ant2 (due to external source) but not from any other cause. According to the established EM theory of the Faraday shield, as demonstrated in Figure 1(a), charges should rearrange in such a manner that the incident electric-field component inside the enclosure is canceled out [5,6]. Therefore, irrespective of the grounding state of the Faraday shield, the resultant electric field should be zero inside according to the classical theory.

The penetration of EM energy through the wall of the CuCyE can be studied by Eq. 3. The effectiveness of shielding is calculated using Eq. 6 with the parameters given below.

Parameters to calculate shielding effectiveness:

$$\mu_0 = 1.256637 \times 10^{-6}\ H.m^{-1}$$
$$\varepsilon_0 = 8.854 \times 10^{-12}\ F.m^{-1}$$
$$\mu_{Cu} = 1.256629 \times 10^{-6}\ H.m^{-1}$$
$$\sigma_{Cu} = 5.8 \times 10^{7}\ S.m^{-1}$$
$$f = 150\ MHz$$
$$t = 1mm$$

The calculated effectiveness is approximately

$E_t = E_i 1.6 \times 10^{-85}$.

This calculation shows that the electric field transmitted through the CuCyE is negligible. Therefore, according to the established theory of EM waves, the CuCyE should shield both the electric and magnetic fields. Thus, no current is induced inside the CuCyE. Both the preliminary and detailed experiments of this article empirically demonstrate the penetration of the energy field, which induces a current in a conductor (antenna) placed inside the Faraday shield (CuCyE).

In Exp. II(a), the CuCyE geometry and antennae were simulated using HFSS. HFSS models an EM system through Maxwell's equations and solves the equations using finite-element methods

[39]. The induced voltage signals of the antennae were estimated relative to the outer screen of the coaxial cables, which is connected to the oscilloscope $ground_{CH1}$ and $grount_{CH2}$. The simulated electric field across the gap was approximately 52 V/m (Figure 8(a)) when there is no shielding. Therefore, the average voltage difference across the gap (space between XX' and YY' in Figures 7(a) and 8(a)) is 520 mV (52 V/m X 0.01 m). When no shielding was used, an 800-mV signal is observed experimentally in both antennae (Figure 5(a) and Table II). The signal measured in the experimental setup over the simulation shows a higher voltage, which could be accounted for by the constructive interferences caused by multiple reflections in the general indoor environment at the antennae. Nonetheless, both the simulation and experimental results show a similar level of signal detected in the antenna. Moreover, the HFSS simulation of the two enclosed antennae shows that induced voltages are nearly zero on both antennae (XX' and YY' in Figures 7(b) and 8(b)). Contrary to this simulation result, the experiment shows a voltage induced at Ant-1 (gap XX') when antennae are enclosed. This induced voltage is greater than the measured voltage at the same antenna without the enclosure: 1460 mV when shielded versus 816 mV when unshielded (Figure 5(a), Figure 5(b), and Table II). Therefore, the simulation based on Maxwell's equations fails to replicate the field within the CuCyE that is detected through experimental observations.

One may argue that the measured voltage at Ant-1 is due to the possible capacitive coupling between the field across the hole (used to mount BNC 1 in the CuCyE) and Ant-1. The impact of the capacitive coupling between the hole and Ant-1 was evaluated by inserting the coaxial cable of Ant-1 further into the enclosure (Supplementary data Note 7. Sup. Fig. 7). No change in measured voltage was observed, indicating that capacitive coupling does not occur. Another alternate explanation could be that the holes used to insert antennae result in an imperfect Faraday shield. The diameter of the hole in the CuCyE is 10 mm, and the wavelengths used in this experiment is 2000 mm. Therefore, the incident waves do not fall into categories of high- and intermediate- frequency regions relative to the dimensions of the hole [18]. Further, it is possible to approximate the enclosure as a cylindrical resonant cavity and the aperture as an iris with a hole for exciting the cavity [19]. The dimensions of the cavity (420-mm length and 50-mm diameter) are small compared to the wavelength of the excitation signal (2 m) [40,41]. Hence, the enclosure cannot be considered as a resonant cavity [42,43], and the field detected inside cannot be considered to be originating from a resonant cavity. If the enclosure were a resonant cavity, the measured voltage should always be less than the excitation voltage [44]. However, according to Table II, the measured voltage at the antenna within the enclosure is nearly twice the measured voltage without the enclosure.

In order to avoid the possibility of mutual interactions between Ant-1 and Ant-2, the two antennae are de-coupled by physically shielding them with two separate copper enclosures in different configurations, as shown in Supplementary data Note 4 and Note 5. No change in results were observed. An experimental setup consisting of several isolated concentric copper cylinders (6

cylinders) with an antenna inside the innermost cylinder also showed that the field cannot be blocked even by multiple conducting shields (see Supplementary Note 3).

The eddy current [5] is a mechanism that can be used to explain the reduction of the time-varying magnetic field inside a Faraday shield. When EM waves come in contact with the Faraday cage, they create a current due to the conductivity of the conductor, known as an eddy current. Note that a changing magnetic field always generates a current in conductors; this phenomenon is called EM induction [6]. These eddy currents, in turn, create time varying magnetic fields that oppose the field of the incoming EM waves (Figure 1(b)). Hence the time varying magnetic fields are blocked from entering the interior [7]. The depth up to which the eddy current exists is called the skin depth. With a high electrical conductivity, when the frequency of the incident wave increases, most of the EM energy is converted/dissipated as eddy current near the surface of the metallic enclosure. The eddy currents generate an opposing magnetic field, canceling the incident magnetic field. This causes negligible EM fields inside if the skin depth is less than the thickness of the enclosure. The calculated skin depth δ for copper is 6.54 μm at 151.880 MHz (Eq. 8). This length is much less than the thickness of the copper sheet (1.2 mm).

In Exp. II(b), a voltage is observed because of an induced current in the loop antenna. The measured voltage in the loop antenna is considered as the electro-motive force (EMF) due to the current induced by the magnetic fields. The loop antenna is sensitive to the magnetic field but not to the electric field [45]. The measured voltage across a 50-Ω resistor was only 288 mV without the CuCyE. With the CuCyE, the induced voltage was increased to 488 mV (see Figures 5(c) and 5(d)). It is assumed that the output voltage of the loop antenna is proportional to the magnetic field of the incident EM wave. According to established EM theory for Faraday shields, the magnetic field should be zero or significantly less than the induced signal without the enclosure. However, we have experimentally observed induced currents in the loop antenna, which indicates the presence of a magnetic field inside the Faraday shield according to the classical EM theory. The penetration of the time-varying electric and magnetic fields (EM field) in the CuCyE cannot be justified with the classical theory of Faraday shields, Gauss's law (Eq. 2), Maxwell's equations (simulations in Figure (7)), EM shielding (Eq. 3), the skin effect (Eq. 8), or a resonant cavity [19].

It is apparent that the results observed in this study cannot be accounted for by the present EM theories. Therefore, a need arises for a new model that consistently explains the experimental observations. Based on our results, it is clear that a self-propagating energy wave in free space propagates through the conductors and produces an electrical current in the CuCyE as well as in the antenna regardless of the presence of the Faraday shield (Figure 4(a)). The signal is created in the oscilloscope when the self-propagating energy or the electrical current from the antenna flows through the oscilloscope to the oscilloscope ground. Therefore, we hypothesize that the energy propagates inside the conductor as it does through free space.

PART B

Several experiments conducted to investigate the nature of propagation of electro-magnetic waves in Faraday shields, were discussed in the previous sections of this manuscript. The experimental evidence revealed some contradictory behaviors of electro-magnetic waves with the existing theories that govern over the wave propagation. Hence the need for a new model to explain these observations emerged. This section presents an alternative heuristic model that can explain the observations of the previously mentioned experiments.

Spin is an important intrinsic property of elementary particles and plays a fundamental role in the interactions among them. All fundamental interactions are spin dependent. In electric and magnetic interactions, similar to positive and negative charges or north and south magnetic poles, parallel spins repel each other and anti-parallel spins attract each other [46]. In contrast, in gravitation, a pair of particles with parallel spins are attracted to each other [47-50]. In quantum electrodynamics (QED), spin exists in fermions/bosons [51,52].

The new model proposes that the propagating field contains energy in a form similar to the conventional rotational or Spin energy fields [53-55], rather than electric and magnetic fields, which suggests that spin represents the energy. Despite the scale of size, any system is associated with spin, which could be considered analogues to the matter wave or de Broglie wavelength [56]. Any system irrespective of the size can produce energy fields in free space. Owing to this assigned nature, an alternative view is to describe the phenomenon as an Intrinsic Spin-energy (of a system) and Intrinsic Spin-energy field (in a field). In this model, new entities named "I-Spin-energy" (ISpE) and "I-Spin-energy-field" (ISpEF) are defined. ISpE is not merely the rotational Spin energy of classical quantum mechanics, but rather an alternate concept in which an infinite number of spins is permitted. ISpE represents the classical term energy, and ISpEF represents an alternative to the EM field of the classical theory. Based on the observations and results of the above experiments, the following postulates are made.

Intrinsic-Spin Energy (ISpin Energy)

The main postulates of the hypothesis are as follows.

P1: Any particle or object has a its own spin associated with it, which represents its intrinsic energy (I-Spin-Energy) of the entity.

P2: The I-Spin energy inherent in the entity creates an I-Spin energy field (which is different from the classical electromagnetic wave presently established) about it.

P3: The direction of the propagation of the I-Spin-energy-fields is always normal to the I-Spin axis of the entity.

P4: Whenever an entity exists in a constant spin state, the resulting I-Spin-energy-field would be static (unvarying).

P5: An I-Spin-energy-field may be located in space even though an entity generating it may not be evident.

P6: An entity, I-Spin or I-Spin-energy-field, is capable of simultaneously existing in infinite numbers of spin states.

P7: Two main I-Spin patterns are recognized relative to the observer as

- The δ-spin (dextro or right or clockwise spin)
- The λ-spin (laveo or left or anti-clockwise spin)

P8: Entities producing identical spins at a given instant, attract each other while those with non-identical spins repel each other.

P9: However, the I-Spin field is a state of flux and as a result the spin state keeps constantly changing.

P10: The mutual repulsion between the δ- and λ –fields, at the generation, is the basis of initiation of the transmission of energy through free space.

P11: Any I-Spin energy field exist in free space can impart its energy to any other particle it encounters in free space.

Detailed description of postulates.

Postulate 1,2,3,4,5

The energy of each and every entity/particle is represented by its ISpin. When a particle spins, it creates a field around and normal to the spin axis of the particle. For a constant spin, this would be a static ISpin-energy field. This field uniquely represents the energy of the particle. An energy field can exist with or without the association of a particle.

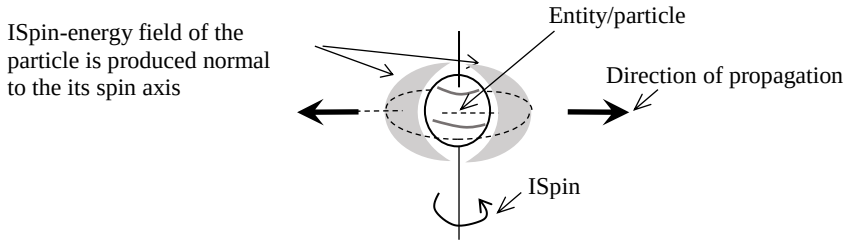

Figure 11. Postulate 1,2,3,4,5 : The physical representation of ISpin energy of a particle that produces an energy field surrounding it.

Postulate 6

ISpin-energy or ISpin-energy field can simultaneously have an infinite number of degrees of freedom for spin.

An infinite number of ISpin axes can exist, and for each axis, an infinite number of ISpins can exist. The total ISpin-energy in the particle creates and emits a unique corresponding ISpEF that contains all ISpin information, similar to white light, which contains information on all colors etc, [57].

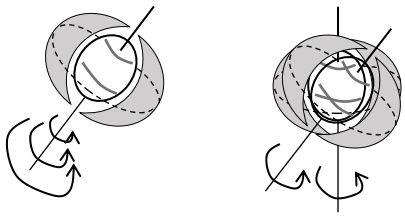

Figure 12. Postulate 6: An entity is capable of existing in an infinite number of ISpin states, hence ISpEFs.

Postulate 7

Consider a situation of two identical particles in all aspects, having the same ISpin axis (Figure 13) but with opposite spins to each other. These two particles create two ISpin energy fields with exactly the same in magnitude but opposite in direction of spin to the observer (right-handed spin field (δ-spin)) and left-handed spin field (λ-spin).

δ-spin and λ-spin energy fields are sequentially originated from a particle if the particle sequentially switches its spin clockwise to anticlockwise.

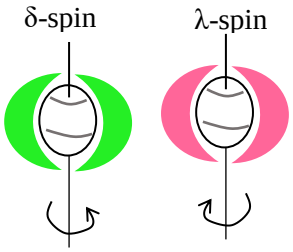

Figure 13. Two particles create two ISpin energy fields with exactly the same in magnitude but opposite in direction of spin to the observer (right-handed spin field (δ-spin)) and left-handed spin field (λ-spin). For the convenience, δ-spin-fields represents in green and λ-spin- fields represents in red.

Postulate 8

For two identical (coherent) ISpin-energy fields attract each other. The difference in ISspin causes a repulsion between them.

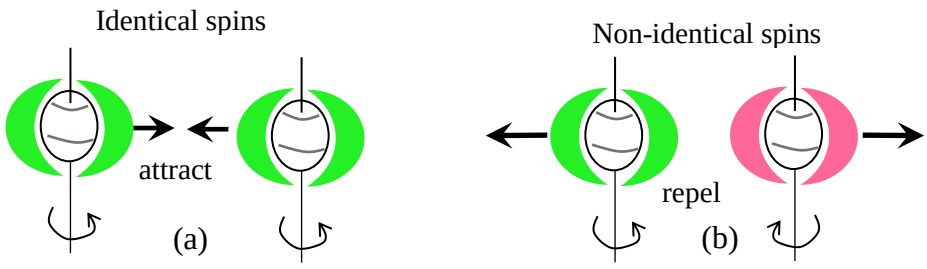

Figure 14. Postulate 8: Interactions between two ISpin-energy fields. (a) Energy with the identical ISpin attracts, and (b) non-identical spins repel each other.

Postulate 9,10

However, the I-Spin field is a state of flux and as a result the spin state keeps constantly changing. The mutual repulsion between no-identical ISpin fields, at the generation, is the basis of initiation of the transmission of energy through free space.

The repulsion between consecutive fields (Figure 14(b)) created in an entity/particle due to the change of its ISpin, initiates the energy fields moving outwards from the origin. As shown in Figure 15, the initially produced δ-spin-field is pushed outward by the subsequently produced λ-spin field.

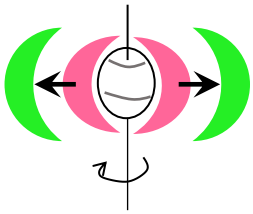

Figure 15. Postulate 8,9: Initiation of propagation of energy in free space. The traveling energy is initiated by the repulsiveness of the consecutive energy fields which are non-identical, produced at the entity with varying spin. For example, the initially formed δ-spin-field is driven outwards by the subsequently formed λ-spin-field.

In the Ispin field, energy is transmitted in the form of δ- and λ-field as against the EM wave of classical theory.

Hence, a field-train carrying energy in free space is formed.

The magnitude of ISpin in a particle (or corresponding ISpEF) corresponds to the amplitude of the classical wave. The period of oscillation of the classical wave is interpreted here as the time of one complete spin cycle containing both δ-spin and λ-spin of the particle producing one energy cycle (unit cycle) in ISpin.

Postulate 11

Any I-Spin energy field created by a particle can impart its energy to any other particle it encounters in free space.

The rotation of ISpin of entity X (Figure 16) produces alternating ISpEFs, and these ISpEFs move away, as shown in Figure 16. These ISpEFs induce corresponding ISpins when they encounter entity Y on its path, as shown in Figure 16. When an entity is exposed to δ_0 (not shown but ahead of λ_0), it absorbs the energy and spins accordingly. Then, the particle Y simultaneously re-emits the same/identical energy to free space as a ISpEF, δ_{00}), but with a delay due to the interaction. The delay depends on the properties of the interacting entity.

Note; Particle "X" is a hypothetical particle that does not exist. All particles act as a receiver and transmitter as the particle "Y".

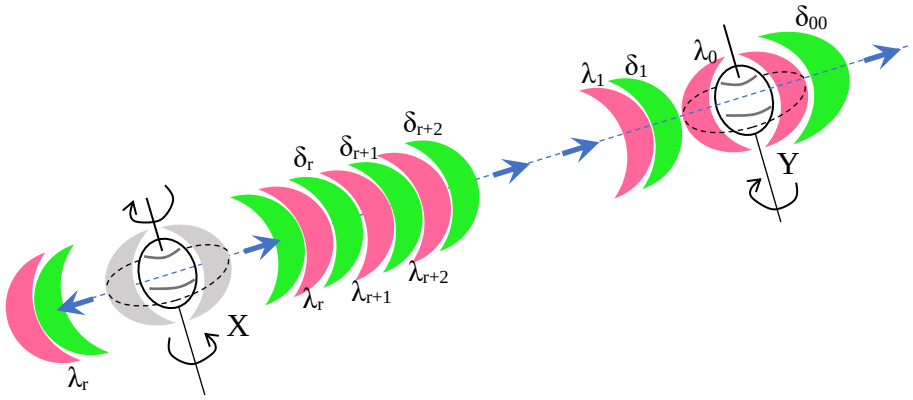

Figure 16. Postulate 10: ISpin-energy field propagating through and the interaction of matter in free space. entity Y absorbs energy δ_0 (not seen but ahead of λ_0) from the incoming ISpEF. This causes to entity Y to spin and simultaneously produces its own ISpEF (δ_{00}). The particle relays energy by receiving and re-transmitting the ISpEF. However, the next approaching energy field has the opposite ISpin (λ_0), which pushes away δ_{00} as it propagates continually after emanating from the source.

However, this ISpEF (δ_{00}) produced by Y is pushed away by the subsequent ISpEF (λ_0: red field in Figure 16) owing to the repulsive forces (postulate 8). This is how the ISpEF propagates

continually forward direction after it emanates from the source. The wave nature was first postulated by C. Huygens, who theorized that light propagates as a wavefront [58]. He further explained that, at any given instant, each point on the wavefront is the origin of a secondary wave that propagates outwards as a spherical wave. The secondary waves then combine to form a new wavefront. However, Huygens principle does not explain the unidirectional propagation of waves; according to Huygens' theory, a backward wave should be formed in the reverse direction [58,59]. Formation of backward wave was omitted in Huygens' theory [60]. However, postulate 11 in the ISpin-energy model explains; once an energy propagation direction (δ-/λ- field direction) is established, it continues to propagate in the same direction though the ISpin-field-train may transfer its energy into other particles (messenger particles) encountered on its way, thus there is no possibility of the reversing of direction of the field-train.

The absolute nature of the ISpin energy fields

It is already established that the ISpin fields brought forward in this model is composed of δ-spin (dextro) and the λ-spin (laveo) as depicted earlier.

In a given ISpin-field-train, the depicted δ-/ λ- fields are their maximum values in magnitudes, but the real picture is that the field-strength continuously keep varying between their maximum values as the spinning entity is constantly changing its character as explained earlier

Hence the field is more exactly represented in a continuously changing nature of its spin and magnitude.

This could also explain the most fundamental experiment in optics [61], double slit experiment (Supplementary data; Note 8) that described the wave nature of the energy propagation, conducted by Thomas Young in 1802.

Energy redistribution or interference is not adequately explained in wave theory [62-64]. According to wave theory, the energy of an EM wave is associated with the electric-field vector *E* and is proportional to $\varepsilon_0 E_0^2 / 2$ (Sup. Fig. 8(c)).

According to the superposition theorem, minima (Zero-energy nodes) or destructive interference occurs in an interference when the electrical vectors of two EM waves are equal and opposite at that node. At the same time, maxima in interference carry an intensity that is four times the original intensity when both beams are coherent and identical in magnitude.

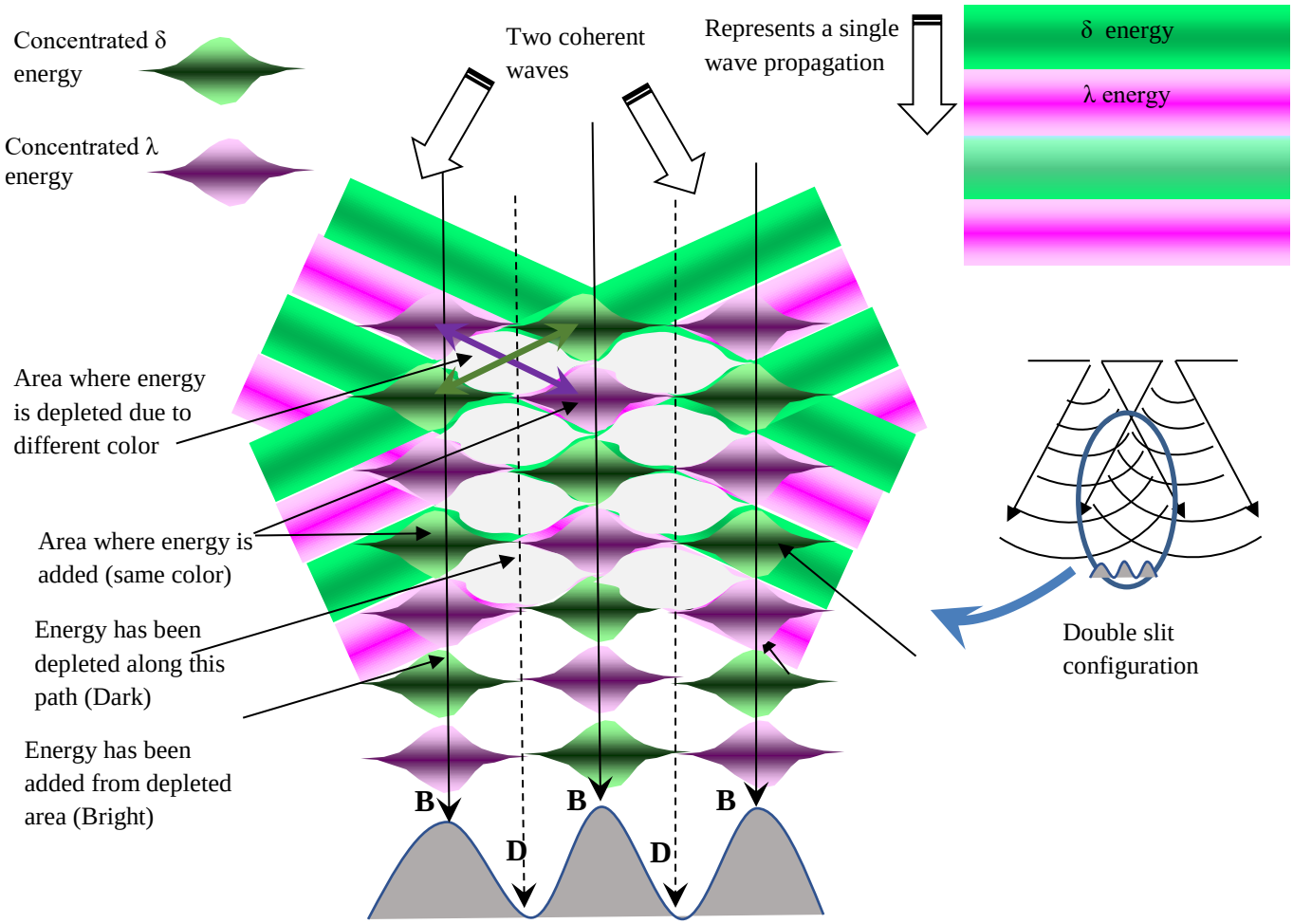

Figure 17. Interference explained using the ISpin-energy wave. The two components of an energy wave are denoted by violet and green. When two coherent waves meet, according to postulate 8 (Fig. 14 (a) and (b)), the area with the same ISpin-energy (same color) attract and different ISpins (different colors) repel each other. This results in energy redistribution or interference.

Although this energy re-distribution is explained mathematically in the superposition theorem [65], it seems that the energy in minima have been depleted towards maxima. Since, according to the classical theory, the two *E* vectors with equal amplitudes have to be present at minima to ensure zero intensities at those regions, we arrive at an important problem as to whether the energies dissociate themselves from their *E* vectors at such zero nodes and moved towards maxima. It is clear that the energy in the dark region D moves/depletes and adds to the maxima, and this movement of energy is not explained in the classical wave theory.

In ISpin-energy theory, when two coherent waves meet, according to postulate 8, same spins (colors) are attracted to each other and form a maxima area), while unequal spins (colors) cannot exist at the same place due to repulsive nature and form a dark area. This results in energy displacement (or in classical theory, energy re-distribution) in interference (see Figure 17). Therefore, the ISpin-energy model can explain the energy displacement/redistribution in interference with greater clarity.

Energy propagates in the free space as well as inside matter. It is assumed that the energy propagates inside the matter similar to the free space. The only difference is the existence of particles in matter compare to free space. The energy propagation inside matter is still governed by all the postulates (especially postulate 11) as matter also contains free space among particles.

The energy propagation occurring in an electric current is defined/interpreted as follows

Definition of electric current according to the proposed model

At any instant, ISpEFs travelling in opposite directions with opposite spins, within a confined space, produce an electric current.

It is defined that, if there exists ISpEFs traveling in opposite directions with opposite ISpins in a conductor at a given time and space (Fig. 18(a)), electric current will be produced. The cross-sectional view of the distribution of ISpEF in a current-carrying conductor is shown in the Fig. 18(b). ISpin field δ- and λ- are assigned to arbitrarily in the figure for the demonstration.

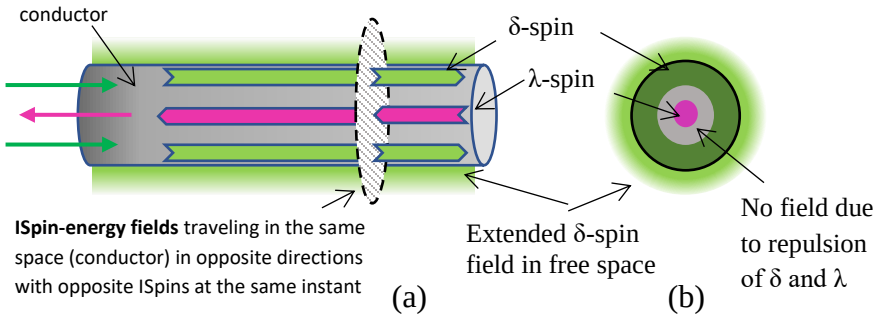

Figure 18. Definition of electric current: (a) Instantaneous view of ISpEFs distributed inside a conductor. The ISpEFs are traveling in the same space in opposite directions with opposite ISpins, Two ISpins are far apart due to its repulsive nature. Most possible existence of mutually repulsive ISpin fields in a conductor is at its circumference and at the center. (b) The cross-sectional view of the distribution of ISpEF in a current-carrying conductor.

Because of the repulsive nature of the two fields, most stable configuration would be, one ISpin energy (either δ or λ) at the surface and the other in the center in the conductor. This is quite analogous to the magnetic field line distribution of a bar magnet or solenoid. The direction of the magnetic field inside the solenoid is opposite to the outside. The ISpin energy flow (or in current in classical terms) in the surface of the conductor could be identified as skin effect in classical definitions.

The proof of the center flow of ISpin energy (or current component in classical terms) can be proven by a separate experiment and this experiment is described in the supplementary data (Note 9).

The forces between two parallel conductors carrying current can also be explained in ISpF (supplementary data Note 10).

The current induced in a conductor due to a propagating ISpF in free space is also described in supplementary file (Note 11).

Next section describes three observations, Exp. II and Supplementary data Note 3 using proposed ISpin model.

Explanation for the experimental observation

Experiment II

In the case of a Faraday shield (CuCyE), in Exp. II, the ISpEF from an external power source propagates as described in postulate 10 and encounters the outermost boundary wall of the CuCyE. Once the boundary is reached, as per postulate 11, the field propagating in free space transfers its ISpE to the particles of the outermost layer of the conducting CuCyE and produces a current. Simultaneously, these particles also re-radiate the energy (Postulate 11) to the spacing among particles within the conducting material, once more as an ISpEF. This process continues as a forward-propagating wave until the ISpin-energy reaches the innermost boundary wall of the enclosure and subsequently to the space enclosed by the CuCyE. Hence, currents are induced when the ISpEF interacts with Ant-1 and Ant-2 inside the enclosure. Previous studies detected zero field inside the enclosure because the measurements are taken relative to the Faraday shield, where the ISpEF produces the same common mode current as in Ant-2 inside, but not because of the absence of the field inside the Faraday shield (Exp. III). The current produced in Ant-1 is free to flow from Ant-1 to the oscilloscope ground (via the oscilloscope electronics) because the oscilloscope ground is floating and free to induce current flow relative to Ant-1.

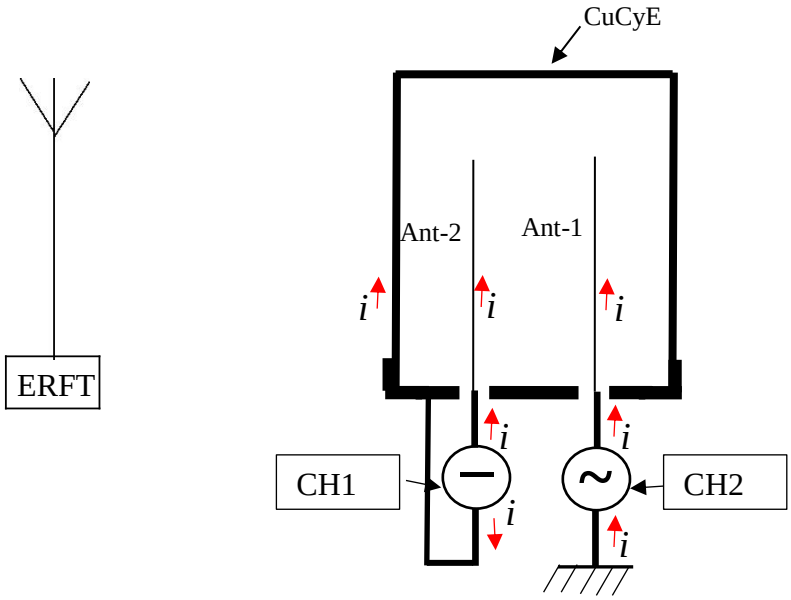

Figure 19. The field produced by the external radio frequency source (ERFS) propagates in free space and transfers its ISpE to the particles of the outermost layer of the conducting CuCyE and consequently in the Ant-1 & Ant-2 producing a current *i*. The resultant current shown in CH1 is zero due to the opposite direction of current flow.

Explanation of multiple enclosures (Supplementary data 3)

The measured amplitude of voltage for each enclosure increases with the number of enclosures of the antenna (Note 3 and Sup. Fig. 3). The measured voltage increases with the increasing diameter of the conductive enclosures. This could be due to an increase in the capturing area or effective cross section for the external field, which increases proportionally with the diameter of the external enclosure. The experiment was conducted in a general indoor environment, resulting in multiple reflections. Therefore, the outer enclosure could also receive energy from multiple directions, which will continue to propagate towards the inside of the enclosures (postulate 11). These two factors together could concentrate (or focus) energy in their inner volumes successively, resulting in a stronger induced current in the antenna (Supplementary data Note 11).

In summary, we have experimentally shown the presence of an induced current inside a perfect Faraday shield. As the classical wave theory fails to explain this phenomenon, an alternative theory (Intrensic-Spin-Energy) was presented. We believe that this novel understanding of the manner in which energy is generated and subsequently transmitted through space would address the properties and aspects of the behavior of EM waves that could not be adequately explained using the classical EM theory. The ISpin-energy model could lead to novel and more effective designs in many applications, such as photovoltaic cells used for solar-energy harvesting, energy storage, EM shielding, and stealth technology.

VI. CONCLUSION

This paper demonstrates the existence of a current in a conductor placed within a Faraday shield, which is in apparent contradiction with the established classical EM theory. An alternative heuristic model was proposed, in which energy propagation is based on two ISpin-energy field components. This proposed model can also be applied comprehensively to the propagation and interaction of energy with matter, including Young's double-slit experiment, which provided the basis for the wave theory of light. A detailed analysis of the proposed theory and how it explains other existing phenomena will be discussed in a separate manuscript.

ACKNOWLEDGEMENTS

Experimental work was conducted at the Department of Electrical and Computer Engineering, University of Manitoba. Dr. Piyadasa was financially supported by the Natural Sciences and Engineering Research Council (NSERC) of Canada. The financial support given by the Harsha Subasinghe and the Codegen International Pvt. Ltd is greatly acknowledged. The author would also like to acknowledge H. Piyadasa for their extensive edits to improve the quality of this manuscript.

REFERENCES

[1] T. Young, Philosophical Transactions of the Royal Society of London **92**, 12 (1802).
[2] M. Planck, Annalen der Physik **306**, 69 (1900).
[3] J. C. Maxwell, *A dynamical theory of the electromagnetic field* (The Society, London, 1865).
[4] J. D. Jackson, *Classical electrodynamics* (Wiley, New York, 1999), 3rd edn.
[5] B. M. Notaros, *Electromagnetics* (Pearson, Upper Saddle River, N.J. ; London, 2011), International edn.
[6] H. W. Ott and H. W. Ott, *Electromagnetic compatibility engineering* (John Wiley & Sons, Inc., Hoboken, New Jersey, 2009).
[7] M. Zahn, *Electromagnetic field theory : a problem solving approach* (Krieger Pub. Co., Malabar, Fla., 2003), Reprint edn.
[8] N. A. Zakaria, R. Sudirman, and M. N. Jamaluddin, in *2008 IEEE 2nd International Power and Energy Conference*2008), pp. 666.
[9] J. H. Wu and J. A. del Alamo, Solid-State Electronics **85**, 6 (2013).
[10] B. J. Lee, P. D. Olcott, H. Key Jo, A. M. Grant, C. Chen-Ming, and C. S. Levin, in *2013 IEEE Nuclear Science Symposium and Medical Imaging Conference (2013 NSS/MIC)*2013), pp. 1.
[11] P. H. Handel and T. F. George, AIP Conference Proceedings **1129**, 491 (2009).

[12] V. Milián-Sánchez, A. Mocholí-Salcedo, C. Milián, V. A. Kolombet, and G. Verdú, Nuclear Instruments and Methods in Physics Research Section A: Accelerators, Spectrometers, Detectors and Associated Equipment **828**, 210 (2016).
[13] H. A. Bethe, Phys Rev **66**, 163 (1944).
[14] G. Cerri, R. D. Leo, and V. M. Primiani, IEEE Transactions on Electromagnetic Compatibility **34**, 423 (1992).
[15] C.-H. L. J.-Z. Lei, and Y. Zhang, Progress In Electromagnetics Research **74**, 85 (2007).
[16] S. Celozzi, R. Araneo, and G. Lovat, *Electromagnetic shielding* (Wiley-Interscience : IEEE Press, Hoboken, N.J., 2008), Wiley series in microwave and optical engineering.
[17] S. J. Chapman, D. P. Hewett, and L. N. Trefethen, Siam Rev **57**, 398 (2015).
[18] A. J. McDowell and T. H. Hubing, IEEE Transactions on Electromagnetic Compatibility **56**, 1711 (2014).
[19] L. D. Smullin, Proceedings of the IRE **37**, 1442 (1949).
[20] A. J. Fresnel, H. H. de Sénarmont, É. Verdet, and L. F. Fresnel, *Œuvres complètes d'Augustin Fresnel: Théorie de la lumière* (Imprimerie impériale, 1866).
[21] G. Kirchhoff, *Zur Theorie der Lichtstrahlen* 1882).
[22] R. S. Longhurst, *Geometrical and physical optics* (Longman, London, 1973), 3d edn., A Longman text.
[23] G. R. Fowles, *Introduction to Modern Optics* (Dover Publications, 1975).
[24] E. Hecht and A. Zaj*ac, *Optics* (Addison-Wesley, Reading, Mass, 1987), 2nd edn.
[25] G. A. Maggi, P. S. Roberto, and V. Volterra, *Sulla propagazione libera e perturbata delle onde luminose in un mezzo isotropo* (publisher not identified, 1871).
[26] R. Kumar, Applied Physics B **90**, 379 (2007).
[27] C. K. Gamini Piyadasa, The European Physical Journal D **64**, 505 (2011).
[28] C. K. G. Piyadasa, Optics Communications **285**, 4878 (2012).
[29] D. J. Griffiths, *Introduction to electrodynamics* (Prentice Hall, Upper Saddle River, N.J. ; London, 1999), 3rd edn.
[30] K. L. Kaiser, *Electromagnetic Shielding* (Taylor & Francis, 2005).
[31] C. R. Paul, *Introduction to electromagnetic compatibility* (Wiley-Interscience, Hoboken, N.J., 2006), 2nd edn., Wiley series in microwave and optical engineering.
[32] T. Williams, *EMC for Product Designers* (Elsevier Science, 2011).
[33] W. H. Hayt, *Engineering electromagnetics* (McGraw Hill, New York ; London, 1981), 4th edn., McGraw-Hill series in electrical engineering.
[34] H. Lamb, Philosophical Transactions of the Royal Society of London **174**, 519 (1883).
[35] L. C. Shen and J. A. Kong, *Applied electromagnetism* (PWS ;

International Thomson Pub., Boston, Mass.

London, 1995), 3rd edn., PWS Foundations in engineering series.
[36] L. T. Gnecco, *The design of shielded enclosures* (Newnes, Boston, Mass., 2000).
[37] C. A. Balanis, *Antenna theory : analysis and design* (Wiley-Interscience, Hoboken, NJ, 2005), 3rd edn.
[38] R. M. Wald, *General relativity* (University of Chicago Press, Chicago ; London, 1984).
[39] M. Kopp, edited by A. LLC225 West Station Square Drive, Suite 200

Pittsburgh, PA 15219, 2009).

[40] Y. J. Xiang Li, Masters thesis in electronic and telecommunications, University of Gavle, 2010.
[41] A. Das and S. K. Das, *Microwave Engineering* (Tata McGraw-Hill Publishing Company, 2000).
[42] D. K. Cheng, *Field and wave electromagnetics : solutions manual* (Addison-Wesley Pub., Reading, Massachusetts ; Wokingham, England, 1989), 2nd ed edn.
[43] M. Fujimoto, (Springer,, New York, 2007), pp. xii.
[44] S. L. Kramer and J.-M. Wang, Nuclear Instruments and Methods in Physics Research Section A: Accelerators, Spectrometers, Detectors and Associated Equipment **423**, 260 (1999).
[45] R. Poisel, *Antenna systems and electronic warfare applications* (Artech House, Boston, Mass. London, 2012), Artech House electronic warfare library.
[46] R. M. Eisberg and R. Resnick, *Quantum physics of atoms, molecules, solids, nuclei, and particles* (Wiley, New York ; Chichester, 1985), 2nd edn.
[47] R. Wald, Physical Review D **6**, 406 (1972).
[48] V. de Sabbata and C. Sivaram, Il Nuovo Cimento A (1965-1970) **101**, 273 (1989).
[49] W. B. Bonnor, Classical and Quantum Gravity **19**, 143 (2002).
[50] J. Steinhoff and G. Schäfer, Physical Review D **80**, 088501 (2009).
[51] A. S. T. Pires, (Morgan & Claypool Publishers, 2014).
[52] M. A. Srednicki, *Quantum field theory*.
[53] R. A. Beth, Phys Rev **50**, 115 (1936).
[54] M. Padgett and L. Allen, Contemporary Physics **41**, 275 (2000).
[55] A. M. Stewart, European Journal of Physics **26**, 635 (2005).
[56] L. de Broglie, Foundations of Physics **1**, 5 (1970).
[57] R. Glazebrook, *Physical Optics* (Longmans, Green, 1886).
[58] C. Huygens, *Traite de la lumiere : où sont expliquées les causes de ce qui luy arrive dans la réflexion, & dans la refraction ; et particulièrement dans l'etrange réfraction du cristal d'Islande* (Chez Pierre vander Aa, Leide, 1690).
[59] O. S. Heavens and R. W. Ditchburn, *Insight into optics* (Wiley, 1991).
[60] T. Freegarde and ebrary Inc., *Introduction to the physics of waves* (Cambridge University Press, Cambridge ; New York, 2013).
[61] T. Young, Philosophical Transactions of the Royal Society of London **92**, 12 (1802).
[62] C. K. G. Piyadasa, Sri Lankan Journal of Physics **6**, 51 (2005).
[63] C. Roychoudhuri, A. F. Kracklauer, and K. Creath, *The nature of light : what is a photon?* (CRC Press, Boca Raton, 2008), Optical science and engineering, 135.
[64] C. K. G. Piyadasa, Optik - International Journal for Light and Electron Optics **123**, 1988 (2012).
[65] G. R. Fowles, *Introduction to modern optics* (Holt, Rinehart and Winston, New York, 1975), 2d edn.

Supplementary Data

Piyadasa et al.

Note 1: Electrically decoupled/isolated oscilloscopes

The electrically decoupling arrangement used to take the measurements of the signals induced in the antennae.

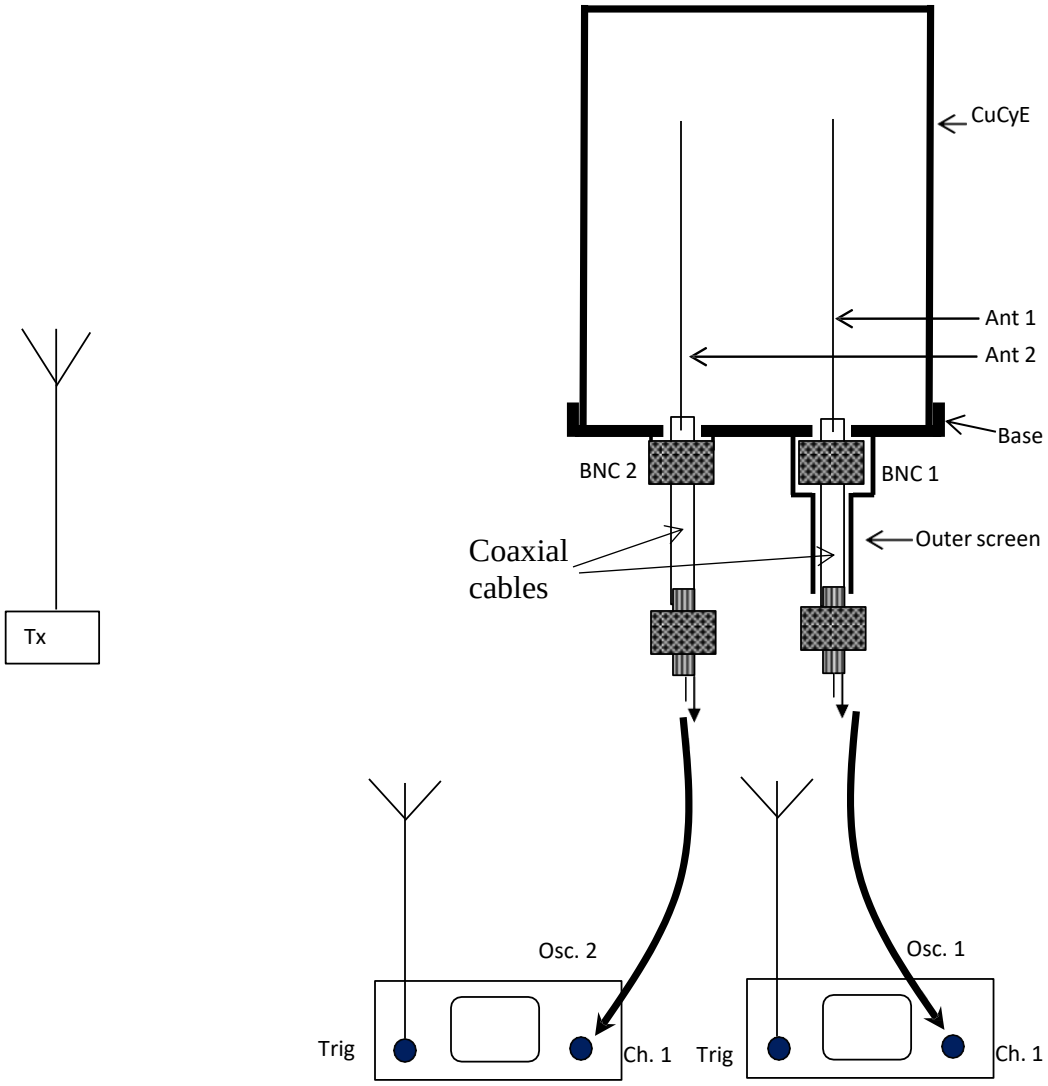

Sup. Fig. 1: Two separate oscilloscopes are triggered with the same radio frequency source used for the main experiment. The induced voltages in the two external antennas trigger the oscilloscopes in order to electrically decouple the two simultaneous measurements.

Note 2: Measurements of Voltages induced in antennae without CuCE

The two voltage measurements of Ant 1 and Ant 2 are taken when unshielded (only the base, no enclosure for the antennae)

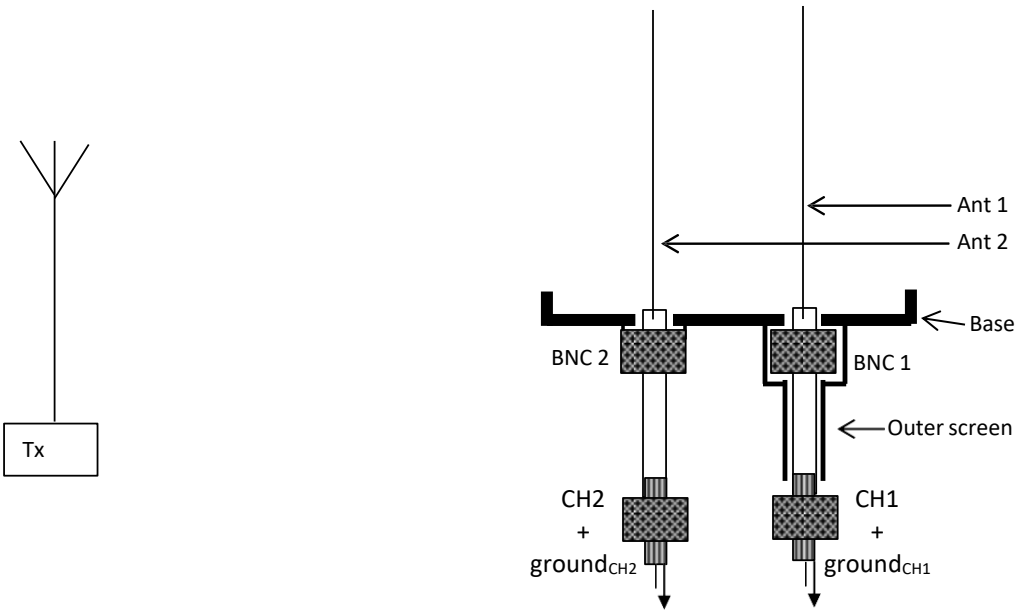

Sup. Fig.2: Voltages induced in Ant.1 and Ant.2 were measured without the CuCyE.

Note 3: Use of multiple conductingenclosures

For further experimenting the hypothesis of absorption and re-radiation of energy, a single antenna was placed inside several enclosures. In this experiment, the antenna was enclosed with multiple enclosures with five different diameters, 15.9 mm, 22.3 mm, 28.8 mm, 54.0 mm and 100 mm as shown in Sup. Fig. 5a. The Mu metal shield was attached to the inside of the copper enclosure with diameter 54.0 mm. The diameter of the antenna was 1.58 mm. The equipment ground was kept unattached to the enclosures. The measured amplitude of the induced signal for each enclosure configuration consisting of the enclosure with the said and all lesser diameters is given in Sup. Fig. 5b.

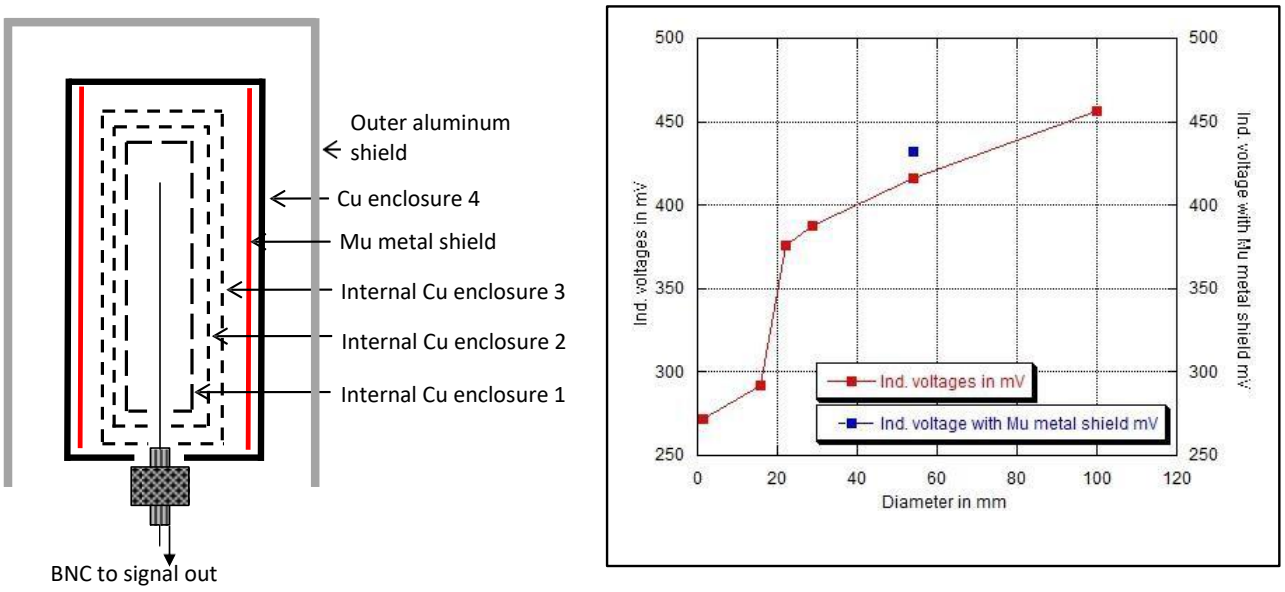

(a) (b)

Sup. Fig. 3: Use of multiple conducting enclosures (a) Enclosure of the antenna with enclosures of five different diameters, 15.9 mm, 22.3 mm, 28.8 mm, 54.0 mm and 100 mm.
(b) The measured amplitude of the induced signal for each enclosure configuration consisting of the enclosure with different diameters.
The induced voltage in the antenna increases with the number of enclosures

Note 4: Decoupling two receiver antennas by two separate copper enclosures

The two antennas of Ex. 1 were separately shielded by another two closed copper cylinders (internal copper enclosures 1 and 2 in Sup. Fig. 3 to check hypothesis of absorption and re-radiation of energy by the particles in the propagation media. Decoupling of any mutual interactions between Ant. 1 and Ant. 2 was also achieved in this experiment. In this experiment, the receiver antennas are placed in a different locations to check the reproducibility in different locations within the enclosure. The induced voltages of Ant. 1 and Ant. 2 due to external EM source, for this configuration are given in supplementary Fig. 6(e).

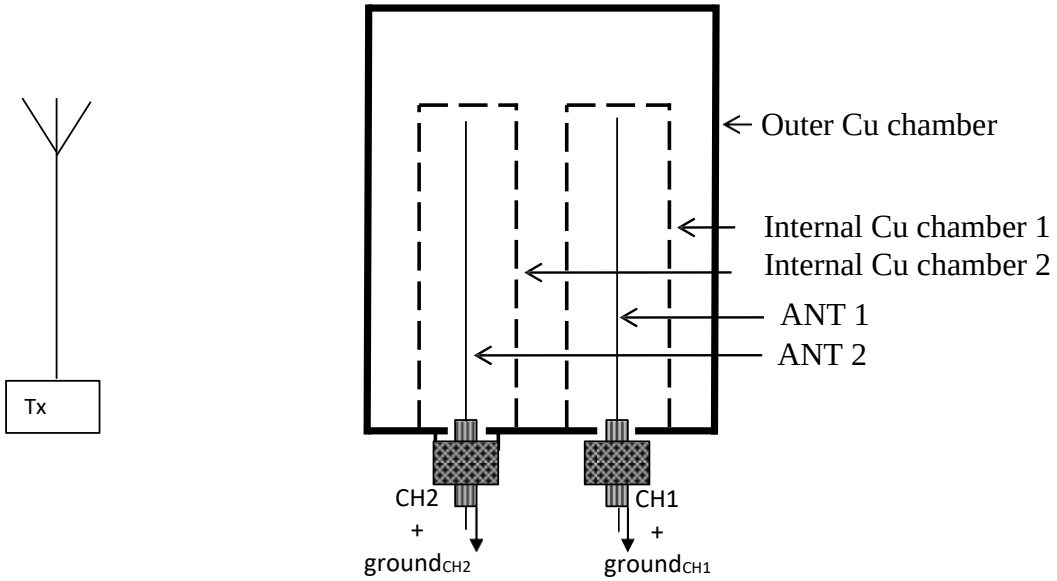

Sup. Fig. 4: Decoupling of the two antennas of Ex. 1 by separately shielding them using two closed copper cylinders (internal copper enclosures 1 and 2)

Note 5: Results of different enclosure configurations

The two antennas were enclosed by different configurations and resultant induced signals as measured by the oscilloscopes are given in Supplementary Fig. 6a to Supplementary Fig. 6e. The reISpEctive configuration for each measurement is shown in the inset.

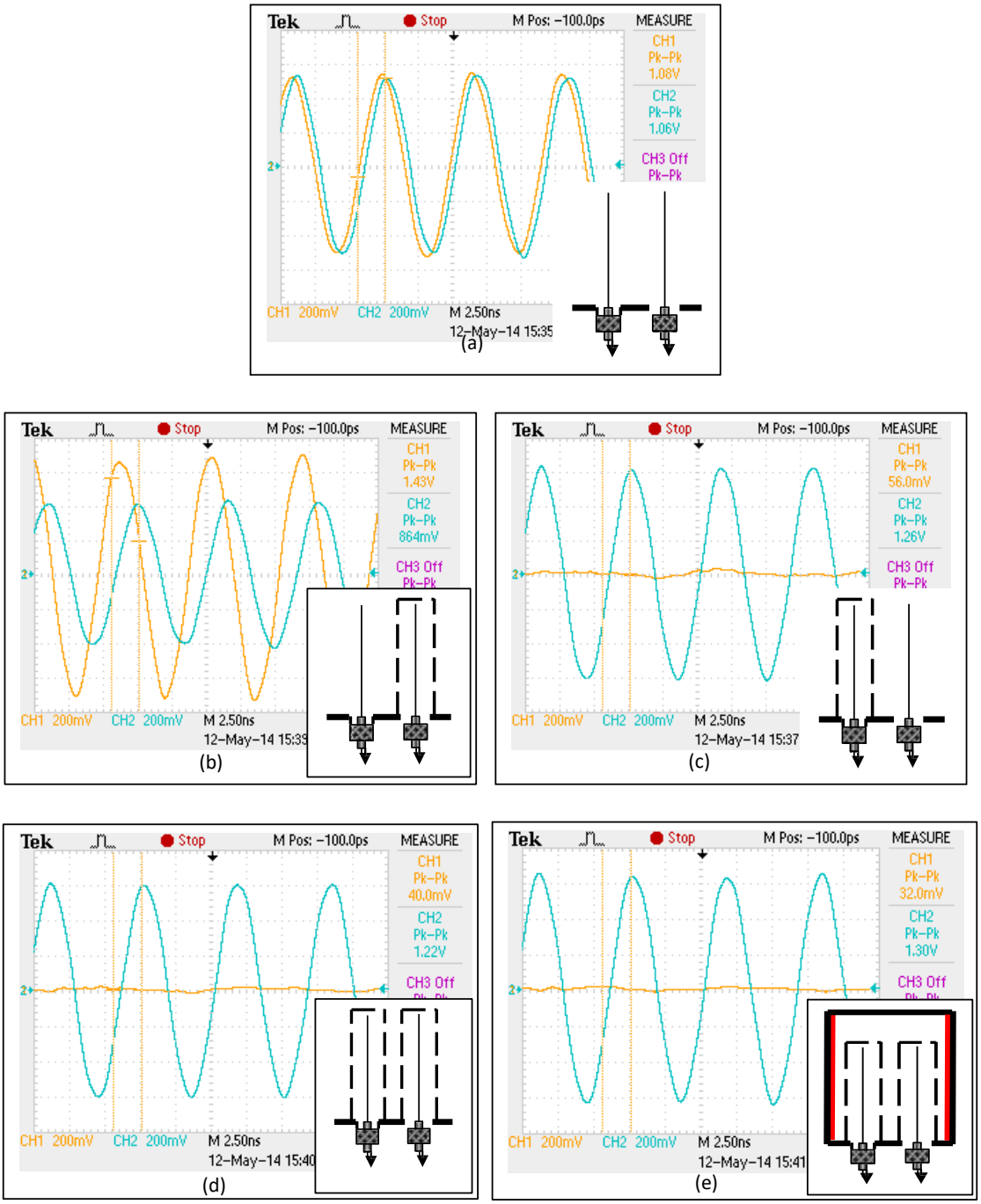

Sup. Fig. 5: The induced signals for different enclosure configurations (a) No enclosures (b) Ant. 1 enclosed. (c) Ant. 2 enclosed. (d) Both antennas separately enclosed without common outer enclosure. (e) Both antennas separately enclosed with common outer enclosure

Note 6: Background noise

The background noise measurements of the coaxial cables used to connect the enclosure and experimental setup are shown in Sup. Fig. 6a and Sup. Fig. 6b respectively. The 151.880-MHz external signal source is in operation when the measurements were taken.

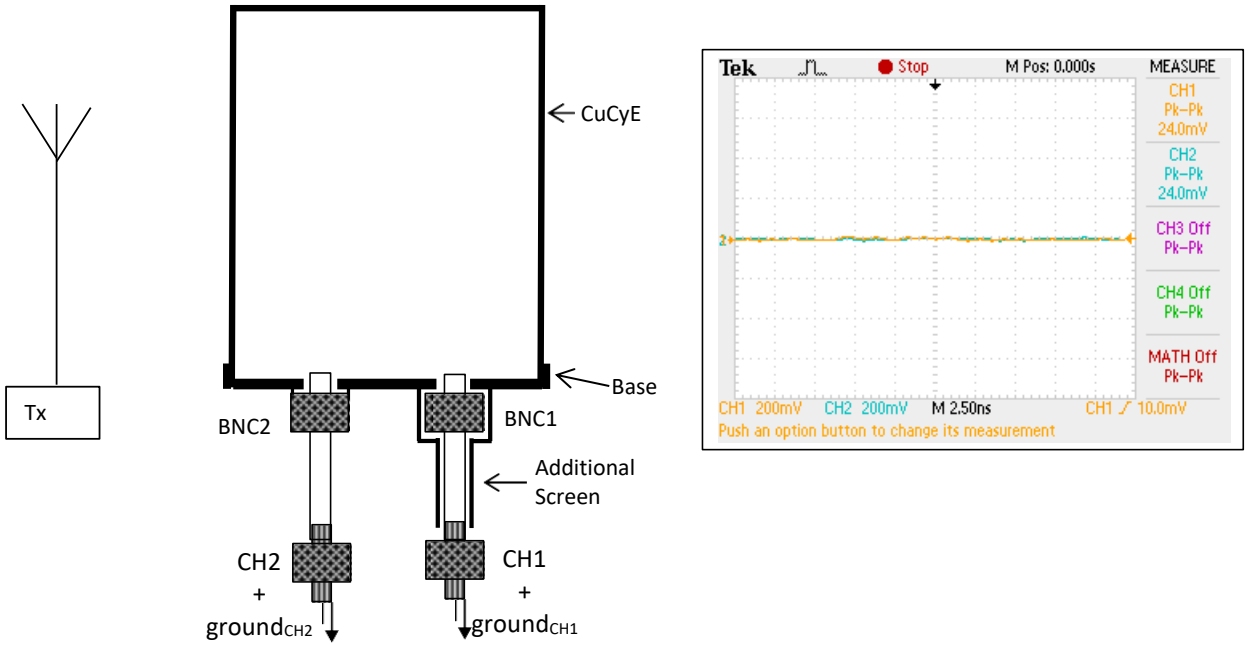

(a) (b)

Sup. Fig. 6: (a) No antennas were connected to the coaxial cables inside the copper enclosure. (b) The reading of the voltage induced in the coaxial cables attached to the oscilloscope. Both channels show ~24 mV.

Note 7: Investigate the influence of the hole A in CuCE on the position of the Ant. 1

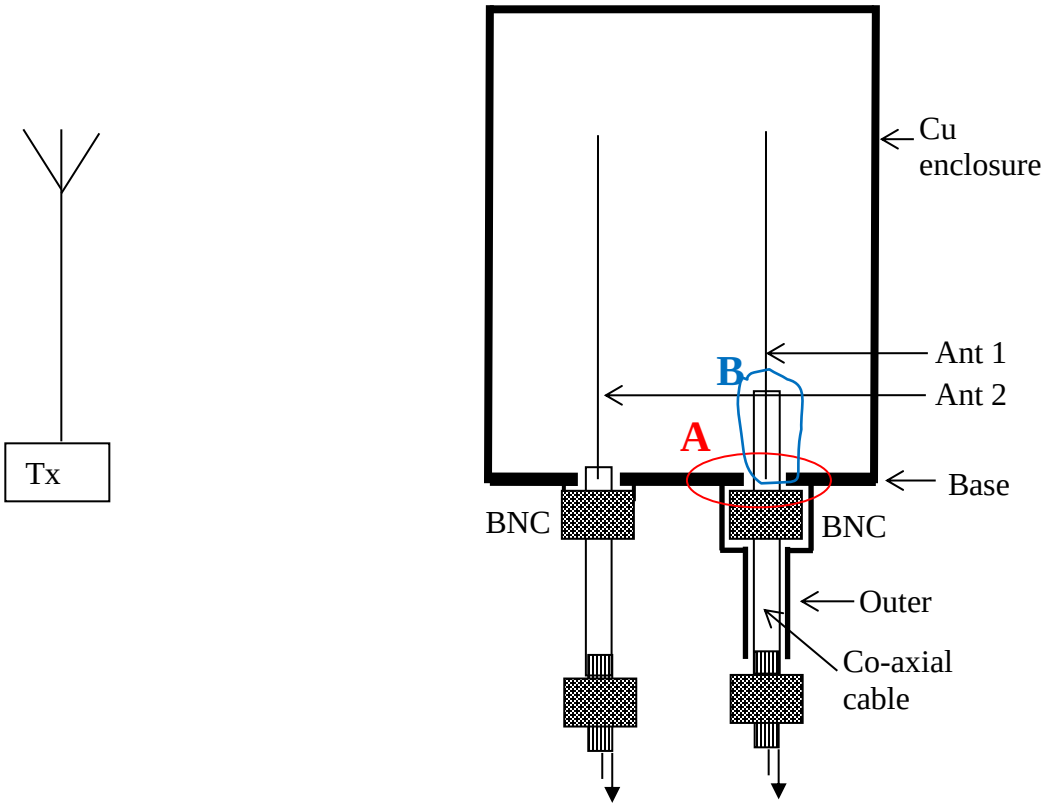

Sup. Fig. 7: Test to whether the induced signal in Ant. 1 is due to a possible field penetration at the hole A. The cable connected to the Ant. 1 is inserted further in the Cu enclosure and this will reduce the coupling between the Ant. 1 and the hole A. B is the extended length of the coaxial cable inside the Cu enclosure.
The Insertion of the cable decreases the capacitive coupling between the Ant. 1 and the Cu enclosure through the hole A. If there is a field at A, then the interaction with the Ant. 1 becomes weaker. The observed signal of Ant. 1 in this configuration didn't change. That implies that there is no influence in capacitive or any other possible coupling between Ant. 1 and the hole of the Cu enclosure.

Note 8: Light interference

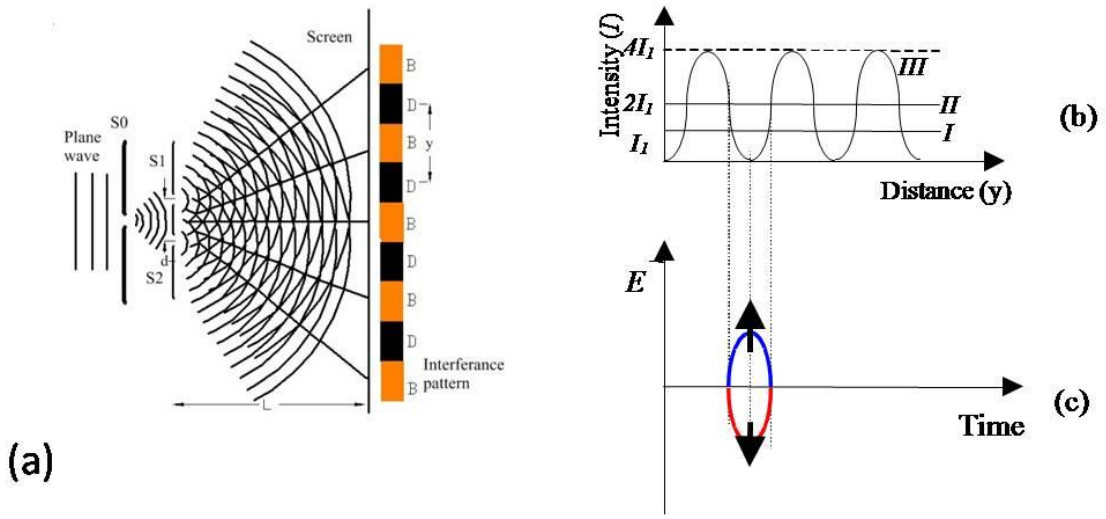

Sup. Fig. 8: (a) Young's double slit experiment and its energy re-distribution. In this, S_0 is a single slit and S_1 and S_2 are double slits. When a plane wave is incident on the slit S_0 it will act as a primary point source and S_1 and S_2 as secondary point sources of light. *B* indicates bright zones and *D* indicates dark zones. The distance between two dark (or bright) fringes in interference pattern is y, λ is the wavelength of the incident wave, *L* is the distance between the plane of the slits and the screen and *d* is the distance between the two slits. (b) Intensity distributions produced by light beams: a single light beam (*I*), double incoherent light beams (*II*) and double coherent light beams (*III*) (c) equal and opposite $\vec{E}$ vectors of two beams produces a null at interference pattern.

Note 9: The proof of two ISpin components in classical current

The experiment was based on the forces between two parallel conductors carrying current. The following factors are well known in parallel wire experiments and general electromagnetic theory,

i) There is an **attraction force** between two current carrying wires when currents flow in **same direction,** Sup. Fig. 9(a)

ii) There is a **repulsive force** between two current carrying wires when currents flow in in opposite direction, Sup. Fig. 9(a)

iii) The force between current **carrying wire and the neutral conducting body is always attractive** due to inductive magnetic field in the wall of the conducting body.

iv) The magnetic field is zero inside the hollow part of the conducting cylinder (Comsol simulation, Sup. Fig. 9(d)) that carrying a uniformly-distributed current I. (an amperian loop encloses no current) and outside the cylinder the magnetic field is the same as that from a long straight wire placed on the axis of the cylinder:

The experimental arrangement is shown in Sup.Fig. 9(b). A solid copper wire was placed eccentrically inside the hollow copper tube as shown in Sup.Fig. 9(b). Currents are sent through the wire and the tube in same and opposite directions.
Comsole simulations shows that the direction of surface magnetic flux inside the tube for both cases (same and opposite direction of current flow) are same and hence only repulsive force must exist between the wire and the inner wall of the tube regardless of the direction of current flow in the hollow tube.

However, the observations show that;

i) There is a repulsion between the wire and the inner wall of the tube when current flows in same direction – *which is opposite to the attraction force between two conductors when current flows in same direction*.

ii) There is an attraction between the wire and the inner wall of the tube when current flows in opposite direction - *which is opposite to the repulsive force between two conductors when current flows in opposite direction*.

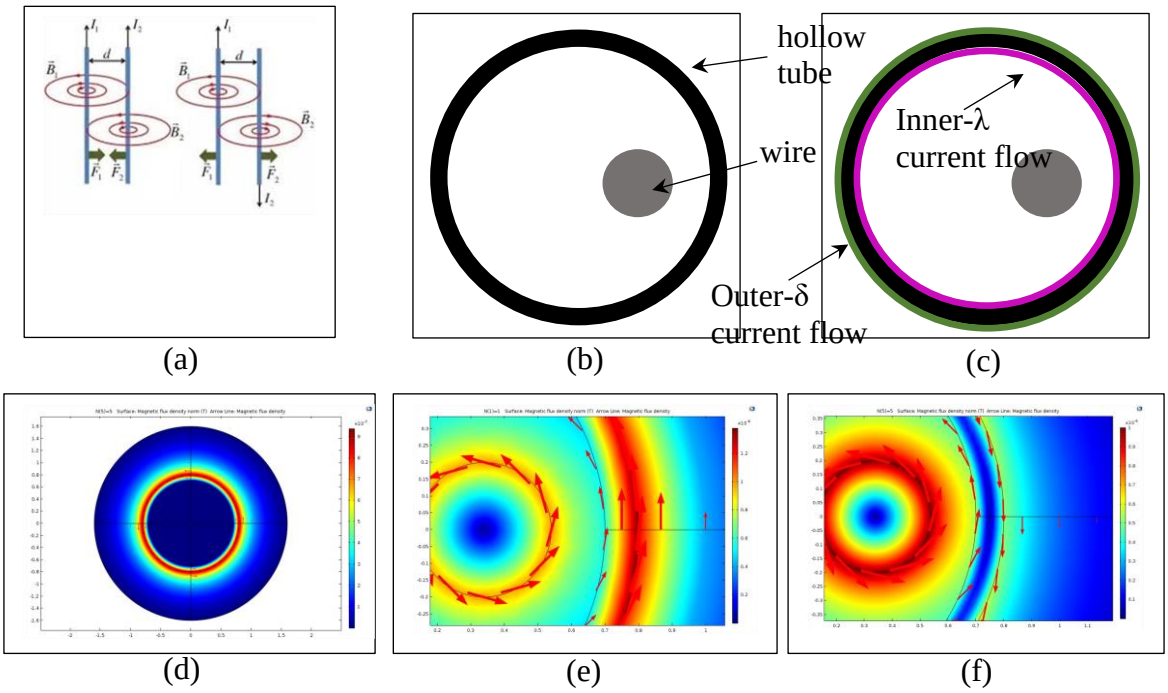

Sup. Fig. 9:

Conclusion:

i) There exists a magnetic field inside the hollow tube although no amperian loop is there which is contrary to the classical theory (amperian law).

ii) This magnetic field inside the hollow tube is opposite to the magnetic field created outside the tube

iii) The current (in classical terms) is responsible for the field inside the hollow tube which causes the magnetic field inside the hollow tube to be opposite to the current that flows outside the hollow tube. In other words, there is a current flow in the inner surface of the hollow tube similar to the current flow in the outer surface. These

currents are flowing in opposite directions and also produces a magnetic field contradicting the amperian law.

Note 10(i): Force between two parallel wires. Two currents are similar and in same directions

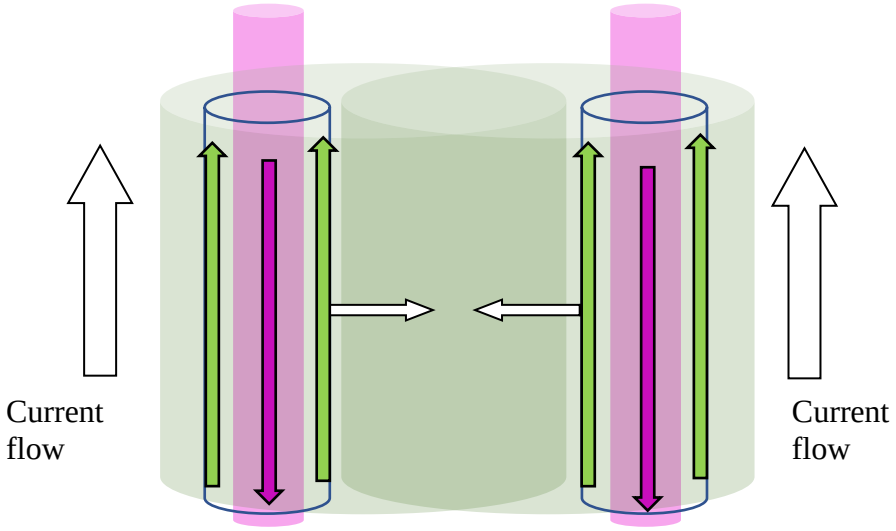

(a)

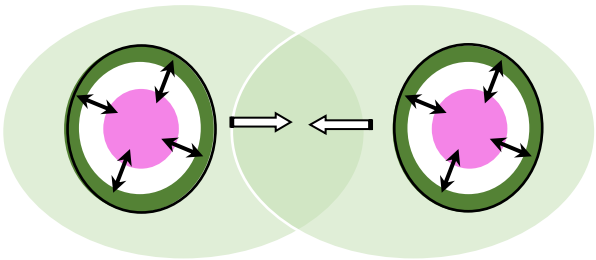

(b)

Sup. Fig. 10(i)

(a) Lateral view of the ISpEF distribution in two parallel conductors. Two currents are similar and in flowing in same direction.
(b) Cross sectional view of the ISpEF distribution in two parallel conductors gives better impression of how ISpEFs are working with two currents that are similar in magnitude and in flowing in same direction. Identical ISpEFs are attractive (postulate 8) and therefore two ISpEFs which are associated with two conductors are also attractive to each other.

Note 11(ii): Force between two parallel wires. Two currents are similar but in opposite directions

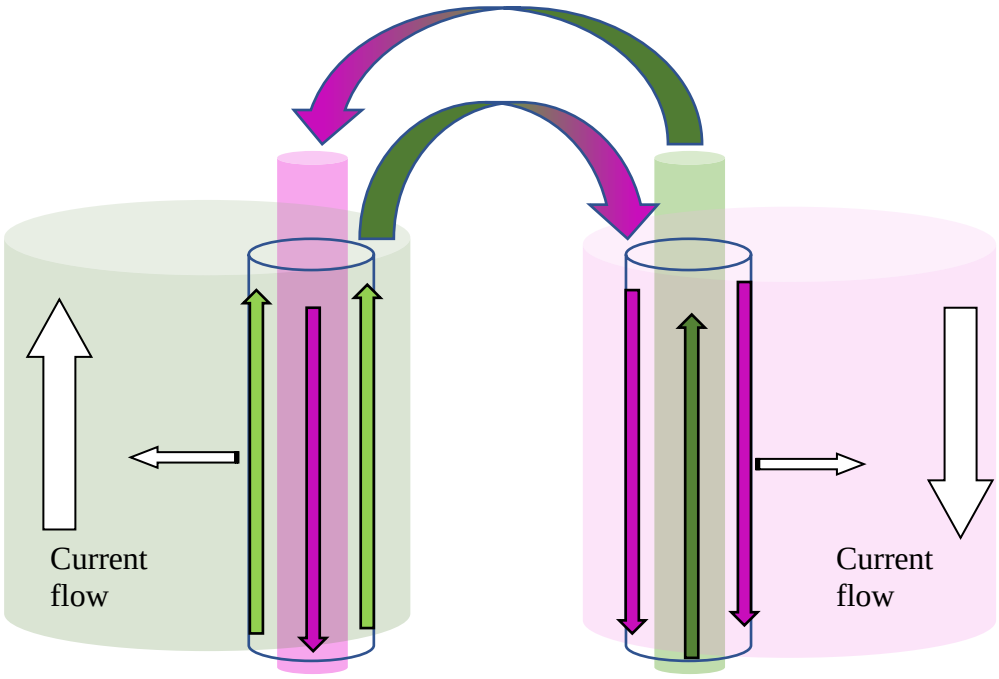

(a)

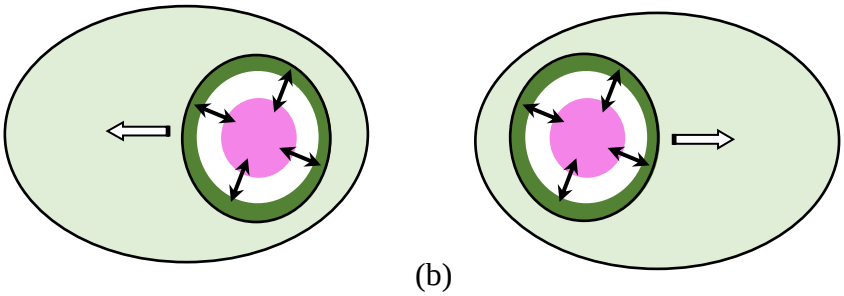

(b)

Sup. Fig. 10(ii)

(a) Lateral view of the ISpEF distribution in two parallel conductors. Two currents are similar and flowing in opposite directions
(b) Cross sectional view of the ISpEF distribution in two parallel conductors gives a better impression of how ISpEFs are working with two currents that are similar in magnitude and flowing in opposite directions. Non-identical ISpEFs are repulsive (postulate 8) and therefore two ISpEFs which are associated with two conductors are also repulsive to each other.

Note 11: A current is formed inside a conductor due to ISpEFs propagating in free space

Sup. Fig. 10 shows how a current is formed inside a conductor by ISpEFs propagating in free space.
A propagating energy wave in free space continually changes the ISpins of the particles of the conductor. When an ISpEF encounters a conductor (arbitrarily selected δ-spin for this demonstration), the ISpE is transferred to the particles outside of the conductor (Postulate 11, Figure 16). The induction in the ISpE of particles in the conductor also initiates the propagation of energy among particles within the conductor along the direction determined by the induced ISpE (similar to the propagation of ISpEF in free space, as there is spacing among particles inside the conductor). If the conductor has a finite length (or a discontinuity), the traveling ISpEFs inside the conductor is reflected, resulting in the production of ISpEFs that travels in the opposite direction with an opposite ISpin similar to the electric current form in the Figure 18. It is defined (in the main text) that, if there exist ISpEFs traveling in opposite directions with opposite ISpins in a conductor at a given time and space, electric current is produced (Sup. Fig. 10).

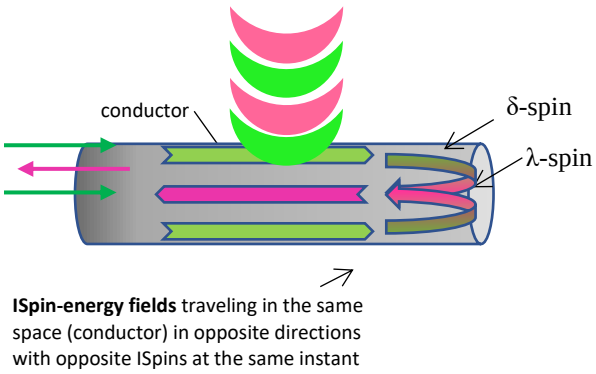

Sup. Fig. 11: Instantaneous view of the induced ISpE/ISpEF distribution inside a conductor due to the incident ISpEF. The induced ISpEF reflected/turned around at the boundary travels back with an opposite ISpin. At an instant of time, if the ISpEFs are traveling in the same space in opposite directions with opposite ISpins, then electric current is produced.

By choosing an appropriate conductor length (for example, integer multiples of a fraction of the wavelength) for a given ISpEF frequency, it is possible to produce two ISpEF components propagating in opposite directions to each other inside the conductor with a maximum intensity/magnitude. This creates a proper alternative electric current (ac/RF) in the linear conductor. To observe the flow of current resulting from ISpEFs effectively, two conditions must be met.

i) First, a conductor having a length of the order of some multiple of a fraction of the wavelength of the incident ISpEF is required.
ii) Second, the conductor must be exposed to both components of the ISpEF sequentially.

The induced current can be detected by placing a suitable current sensor/detector by intersecting the conductor at an appropriate point. When the sensor is placed at the center of the conductor, dividing it into two equal halves, the conductor system is commonly known as a dipole.